


Evolutionary Tuning of Transient Receptor Potential Ankyrin 1 Underlies the Variation in Heat Avoidance Behaviors among Frog Species Inhabiting Diverse Thermal Niches

Shigeru Saito ^{*,1,2,3} Claire T. Saito,^{1,2} Takeshi Igawa,^{4,5} Nodoka Takeda,⁶ Shohei Komaki,⁷ Toshio Ohta,⁶ and Makoto Tominaga^{1,2,3}

¹Division of Cell Signaling, National Institute for Physiological Sciences, National Institutes of Natural Sciences, Okazaki, Japan

²Thermal Biology Group, Exploratory Research Center on Life and Living Systems (ExCELLS), National Institutes of Natural Sciences, Okazaki, Japan

³Department of Physiological Sciences, SOKENDAI (The Graduate University for Advanced Studies), Okazaki, Japan

⁴Amphibian Research Center, Hiroshima University, Higashi-Hiroshima, Japan

⁵Graduate School of Integrated Sciences for Life, Hiroshima University, Higashi-Hiroshima, Hiroshima, Japan

⁶Department of Veterinary Pharmacology, Faculty of Agriculture, Tottori University, Tottori, Japan

⁷Division of Biomedical Information Analysis, Iwate Tohoku Medical Megabank Organization, Disaster Reconstruction Center, Iwate Medical University, Yahaba, Japan

*Corresponding author: E-mail: sshigeru@nips.ac.jp.

Associate editor: Yoko Satta

Abstract

Environmental temperature is a critical factor for all forms of life, and thermal tolerance defines the habitats utilized by a species. Moreover, the evolutionary tuning of thermal perception can also play a key role in habitat selection. Yet, the relative importance of thermal tolerance and perception in environmental adaptation remains poorly understood. Thermal conditions experienced by anuran tadpoles differ among species due to the variation in breeding seasons and water environments selected by parental frogs. In the present study, heat tolerance and avoidance temperatures were compared in tadpoles from five anuran species that spatially and temporally inhabit different thermal niches. These two parameters were positively correlated with each other and were consistent with the thermal conditions of habitats. The species difference in avoidance temperature was 2.6 times larger than that in heat tolerance, suggesting the importance of heat avoidance responses in habitat selection. In addition, the avoidance temperature increased after warm acclimation, especially in the species frequently exposed to heat in their habitats. Characterization of the heat-sensing transient receptor potential ankyrin 1 (TRPA1) ion channel revealed an amphibian-specific alternatively spliced variant containing a single valine insertion relative to the canonical alternative spliced variant of TRPA1, and this novel variant altered the response to thermal stimuli. The two alternatively spliced variants of TRPA1 exhibited different thermal responses in a species-specific manner, which are likely to be associated with a difference in avoidance temperatures among species. Together, our findings suggest that the functional change in TRPA1 plays a crucial role in thermal adaptation processes.

Key words: environmental adaptation, thermal perception, thermal sensors, heat avoidance, heat tolerance, frog tadpole.

Introduction

Environmental temperature is a critical factor for all forms of life, and exposure to extreme cold or heat typically causes deleterious effects. Given these temperature sensitivities, the upper and lower thermal limits for survival will define the thermal niches of each species (Sunday et al. 2011, 2012; Araujo et al. 2013). Moreover, considering that animals have evolved the ability to sense ambient

temperatures to respond behaviorally to changing environments, the evolutionary tuning of thermal perception can also play a key role in the adaptation process (Glauser and Goodman 2016; Angilletta et al. 2019). In such processes, various proteins involved in signal transduction from the periphery to the central nervous system can alter thermal perception (Angilletta et al. 2019). Specifically, recent studies have shown that peripheral thermal sensors play a role in changing thermal perception

© The Author(s) 2022. Published by Oxford University Press on behalf of Society for Molecular Biology and Evolution.

This is an Open Access article distributed under the terms of the Creative Commons Attribution-NonCommercial License (<https://creativecommons.org/licenses/by-nc/4.0/>), which permits non-commercial re-use, distribution, and reproduction in any medium, provided the original work is properly cited. For commercial re-use, please contact journals.permissions@oup.com

Open Access

among species (Bagriantsev and Gracheva 2015; Laursen et al. 2015, 2016; Saito et al. 2016, 2019; Saito and Tominaga 2017; Akashi et al. 2018; Yang et al. 2020). However, the association between thermal tolerance and perception in the context of environmental adaptation remains to be elucidated. Comparative analyses using species harboring similar physiological and ecological characteristics, but occupying different thermal niches, will deepen our understanding of the role of thermal perception in evolutionary adaptation.

Temperature is perceived by peripheral sensory neurons, and signals are transmitted to the central nervous system, where thermal sensation arises. Several channels belonging to the transient receptor potential (TRP) superfamily serve as thermal sensors in primary sensory neurons (Patapoutian et al. 2003; Julius 2013; Laing and Dhaka 2016). These channels are activated by thermal stimuli to trigger neuronal action potentials. Among these channels, TRP ankyrin 1 (TRPA1) and TRP vanilloid 1 (TRPV1) are activated by noxious temperatures, and their activation triggers avoidance behaviors in many animal species (Bagriantsev and Gracheva 2015; Laursen et al. 2015; Saito and Tominaga 2015, 2017). Therefore, the functional properties of these heat sensors potentially help define the habitable thermal niches of each species.

In the present study, we focused on anurans because their breeding seasons and water environments used for spawning vary among species. Therefore, embryos and tadpoles are exposed to diverse thermal conditions even among species with overlapping geographic distributions. We selected five anuran species inhabiting Japan for investigation: *Buergeria japonica*, *Buergeria buergeri*, *Rhacophorus schlegelii*, *Glandirana rugosa*, and *Rana japonica*. *Buergeria japonica* is distributed throughout the Ryukyu archipelago, and the latter four species are widely distributed among the main islands of Japan and are often found in the same geographic regions. *Rana japonica* and *Rh. schlegelii* spawn eggs in late winter and spring, respectively; thus, the tadpoles grow in relatively cool environments. While the breeding seasons of the remaining three species span from spring to midsummer, tadpoles are exposed to heat more frequently. In addition, the water environments utilized by these species are also diverse such as streams, ponds, rice fields, shallow puddles, artificial ditches, and so on, with different thermal conditions. Particularly, tadpoles of *B. japonica* were found in geothermal hot springs and were frequently found in water where temperatures reach 40 °C in a natural hot-spring stream in Taiwan and Kuchinoshima Island in Japan (Chen et al. 2001; Wu and Kam 2005; Komaki, Lau, et al. 2016). *Buergeria japonica* tadpoles generally possess extreme heat tolerance and their upper thermal limit reaches as high as 42 °C (Wu and Kam 2005; Komaki, Igawa, et al. 2016; Komaki, Lau, et al. 2016; Komaki et al. 2020).

To examine the relationship between heat tolerance and avoidance temperatures among five species, we developed novel behavioral assays suitable for amphibian tadpoles. Both heat tolerance and avoidance temperatures

differed among the species. Notably, we observed a larger difference in avoidance temperatures compared with heat tolerance. In addition, the electrophysiological properties of the heat-sensing TRPA1 ion channel were analyzed, which showed consistent functional changes with respect to the thermal niches of the species. Moreover, we found a novel amphibian-specific alternative spliced (AS) variant of TRPA1, which exhibited functional differences in a species-specific manner during the adaptation process. Overall, our findings illuminate the importance of evolutionary changes in thermal perception and avoidance behaviors, which can define thermal niche of a species.

Results

Difference in Heat Tolerance of Tadpoles among the Five Frog Species

We developed a novel behavioral assay to compare the instantaneous heat tolerance of tadpoles and their responses to heat exposure (fig. 1A). Tadpoles were subjected to a temperature ramp (approximately 3 °C/min), and their swimming behaviors and trajectories were observed until reaching to their critical thermal maximum (CT_{max}, defined as the temperature at which tadpoles lose their righting reflex). First, *B. japonica* tadpoles were used for the behavioral assay. Typically, tadpoles swam along the wall of the chamber but showed irregular trajectories upon reaching CT_{max} (fig. 1A and B). The swimming speed of *B. japonica* tadpoles increased slightly before reaching CT_{max} (fig. 1C). The average CT_{max} was 42.6 ± 0.2 °C (*n* = 8) under our experimental conditions and was in the range of previously reported CT_{max} values for *B. japonica* tadpoles (40.6–46.1 °C), although the heating rate varied from 0.16 °C/min to 1 °C/12 h in previous studies (Chen et al. 2001; Wu and Kam 2005; Komaki, Igawa, et al. 2016; Komaki, Lau, et al. 2016).

Behavioral assays were also performed in the four other species, which revealed a gradual shift in the CT_{max} values among the five frog species (fig. 1D–H). As expected, *Ra. japonica* and *B. japonica* tadpoles showed the lowest and highest values, respectively. Significant differences in the CT_{max} values were observed in all pairs of species except for *B. japonica* versus *G. rugosa*, *B. buergeri* versus *G. rugosa*, and *Rh. schlegelii* versus *Ra. japonica* (Supplementary table S1, Supplementary Material Online). The swimming speed of the tadpoles, except for *B. japonica*, rapidly increased prior to reaching CT_{max}, possibly in an attempt to escape from the heat. In contrast, *B. japonica* tadpoles showed only a slight increase in swimming speed even up to CT_{max}, which was clearly different from the pattern seen in the tadpoles of the other four species (fig. 1C–G). These observations led us to hypothesize that *B. japonica* tadpoles do not recognize temperatures close to their CT_{max} as noxious.

A Large Species Difference in Avoidance Temperatures Compared with CT_{max}

To compare heat avoidance of tadpoles among species, we developed a novel behavioral assay. A temperature

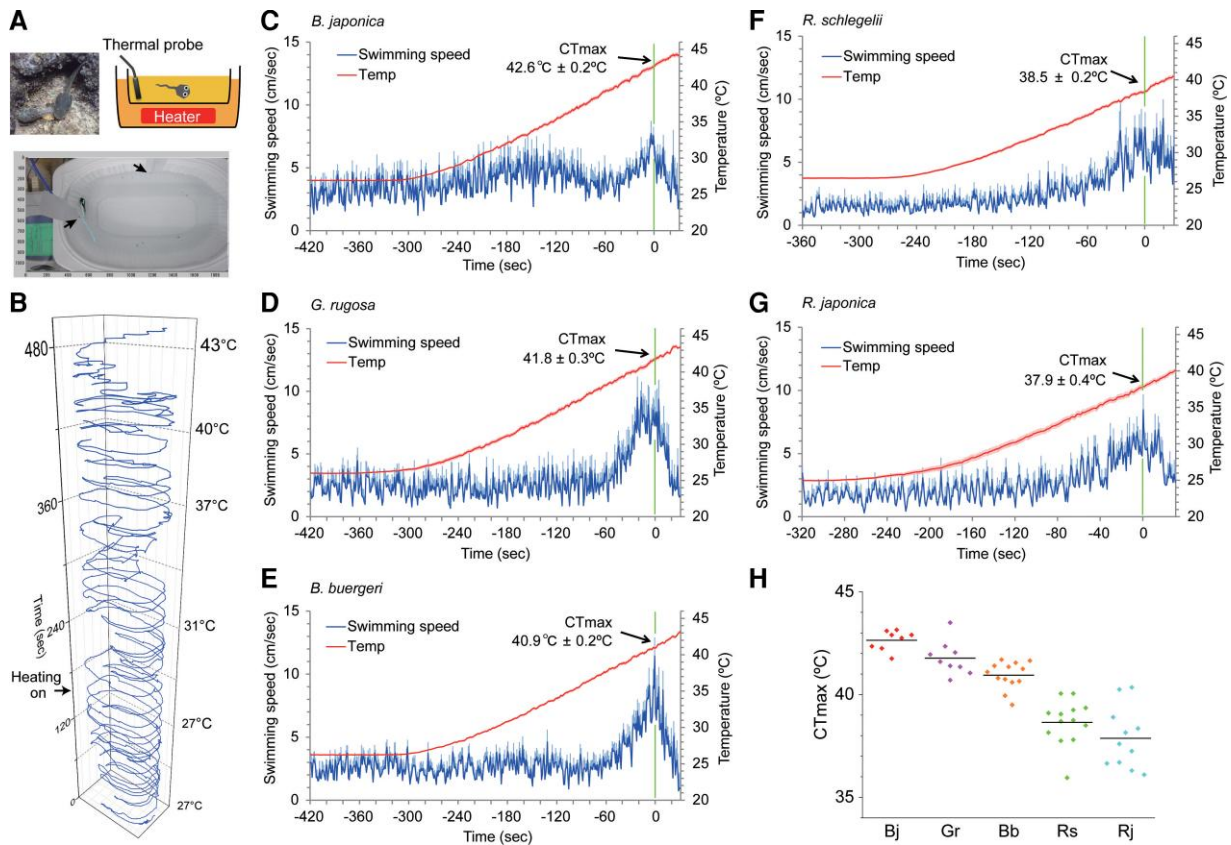


FIG. 1. Behavioral responses of anuran tadpoles to heat. (A) The experimental setup for applying the temperature ramp. An image of *Buergeria japonica* tadpoles (upper left). A schematic structure of the experimental setup (upper right) and a representative image taken from above (below). Arrows indicate the positions of the thermal probes placed on the wall of the chamber. The cyan line shows the trace of a tadpole tracked using idTracker (Perez-Escudero et al. 2014). (B) A representative trace of the movement of *Buergeria japonica* tadpole in response to the temperature ramp. Approximate water temperatures are shown with respect to time (s). (C–G) The average swimming speeds of *B. japonica* (C, $n = 8$), *Glandirana rugosa* (D, $n = 9$), *B. buergeri* (E, $n = 13$), *Rhacophorus schlegelii* (F, $n = 13$), and *Ra. japonica* (G, $n = 11$) tadpoles in response to the temperature ramp. The swimming speeds of the tadpoles obtained from each assay were plotted relative to the time to reach CT_{max} (green line). Error bars for swimming speeds (pale blue) and temperature (pale red) represent the SEM. (H) A graph summarizing the CT_{max} values for five anuran species. The dots indicate the CT_{max} values of individual tadpoles, and the bars represent the average values.

difference was formed between the two chambers connected by a narrow path, and a single tadpole was released. Then, the movement of the tadpole was tracked for 8 min (two-chamber choice assay, fig. 2A and supplementary movies 1 and 2, Supplementary Material online). In the control assay, when the temperature of the entire container was uniformly set to 26 °C, tadpoles were distributed relatively evenly, and they repeatedly entered both chambers (supplementary fig. S1A and B, Supplementary Material online). When one side of the chamber was set to 40 °C (test chamber), the distribution of the tadpoles was skewed (fig. 2B). Even under such conditions, the tadpole repeatedly entered the heated chamber (fig. 2C).

To determine the avoidance temperatures of tadpoles, the temperature of the test chamber was adjusted from 22 °C to 44 °C in a stepwise manner. The avoidance index, ranging from –1 to 1, was calculated by subtracting the time spent in the test chamber from the time spent in the control chamber, and the resulting value was divided by the total assay time. The avoidance temperature was defined as the temperature at which the time spent in

the test chamber was significantly shorter than that spent in the control chamber. The avoidance temperatures among the five species ranged from 28 °C (*Ra. japonica*) to 38 °C (*G. rugosa*) when the tadpoles were reared around 26 °C (fig. 2D). The order of avoidance temperatures among the species, except for *B. japonica*, was consistent with that of the CT_{max} values. In *B. japonica*, the avoidance temperature was 36 °C which was the same as that of *B. buergeri* and lower than that of *G. rugosa*. This result was inconsistent with the field observations, since *B. japonica* tadpoles were found at temperatures above 40 °C in a hot-spring stream on Kuchinoshima Island (Komaki, Lau, et al. 2016; Komaki et al. 2020).

In the above-mentioned assay, tadpoles were collected from a hot spring on Kuchinoshima Island and reared at approximately 26 °C in the laboratory for at least 4 days, which potentially affected their avoidance temperatures. To examine the effect of the rearing temperature on thermal selection, tadpoles were reared at 35 °C, which was slightly lower than the avoidance temperature, for 1 day, and then the two-chamber choice assay was performed.

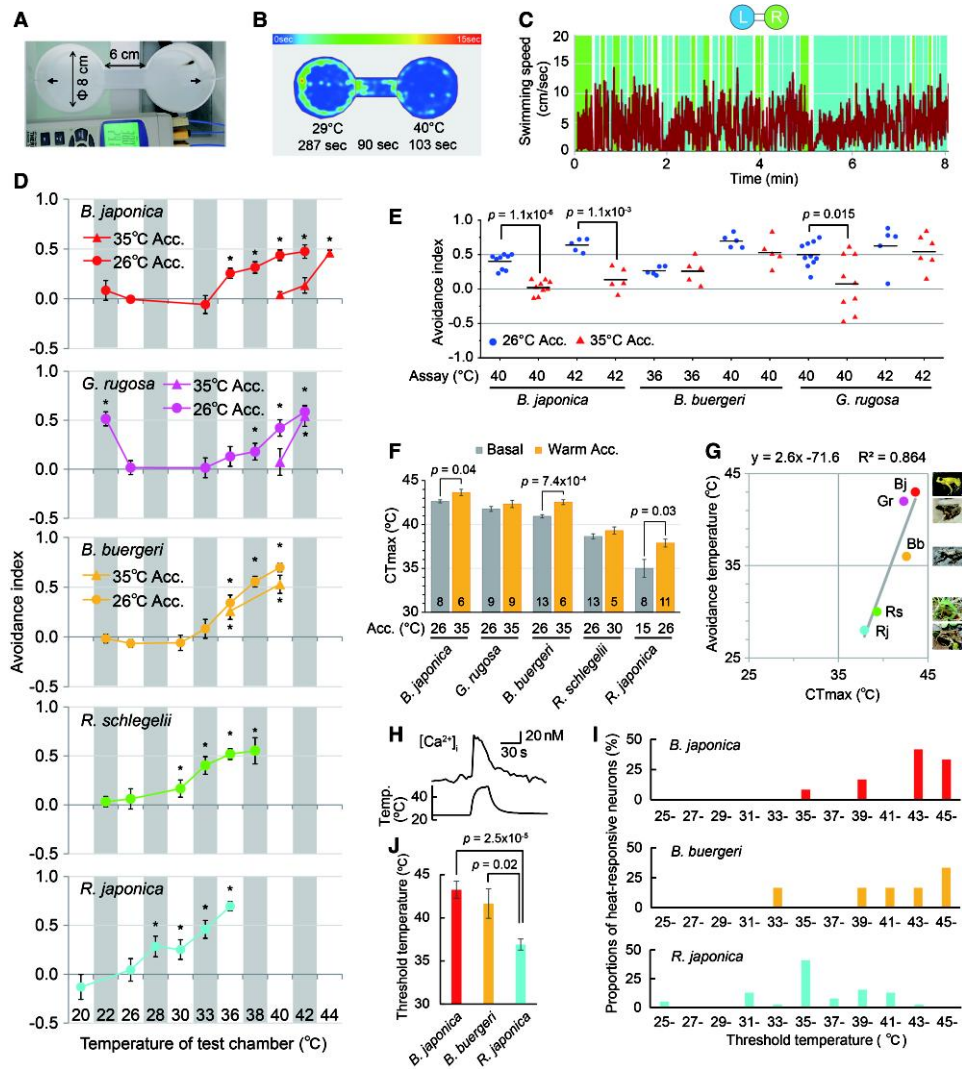


Fig. 2. A greater variation in avoidance temperatures compared with CT_{max} among anuran species. (A) The experimental setup for the two-chamber choice assay. Thermal probes were placed on the wall at each end of the chamber (arrows, see [supplementary movie 1, Supplementary Material](#) online). (B) Representative heat maps showing the distribution of a single *Buergeria japonica* tadpole during the entire assay period (480 s). A temperature difference was formed between the two chambers in the test assay. The time spent in each area during the 480-s period is shown in the representative examples (29 °C vs. 40 °C, see [supplementary movie 1, Supplementary Material](#) online). (C) A plot of the swimming speed of a *B. japonica* tadpole versus time in the representative assay shown in B. The background colors represent the location of tadpoles in each area (left: blue, middle: white, right: green). (D) Graphs summarizing the avoidance indexes of tadpoles for five anuran species under various temperature conditions ($n = 5-15, 5-8, 6-10, 5-9,$ and $10-12$ for *B. japonica*, *Buergeria buergeri*, *Gandirana rugosa*, *Rhacophorus schlegelii*, and *Rana japonica*, respectively). Avoidance indexes of tadpoles acclimated at 26 °C and 35 °C are indicated by the circles and triangles, respectively. Data points marked with asterisks indicate the temperature conditions at which the time spent in the test chamber was significantly shorter than the time spent in the control chamber (Welch's t -test, $P < 0.05$). (E) The effect of warm acclimation on thermal selection in the two-chamber choice assay. Tadpoles were acclimated (Acc.) at 35 °C for 1 day before use in the assay (see [supplementary movies 2 and 3, Supplementary Material](#) online). Tadpoles reared at 26 °C were used as controls. Each data point represents the avoidance index of an individual tadpole. P -values are indicated for cases in which the avoidance index was significantly smaller for warm-acclimated tadpoles than those of control tadpoles. Temperatures in the test chamber are shown below the x -axis. (F) The effect of warm acclimation on the CT_{max} of tadpoles of the five anuran species. The average CT_{max} values of tadpoles reared at lower (basal) and higher (Acc.) temperatures are shown. Note that the acclimation temperatures of *Rh. schlegelii* and *Ra. japonica* were different from those of the other species considering their lower avoidance temperatures shown in D. The number of observations is shown in each bar. Welch's t -test was used for statistical comparisons. (G) A significant (Spearman correlation coefficient 0.929, $P = 0.022$) positive correlation between CT_{max} and avoidance temperature in the anuran species. Note that the avoidance temperature of *B. japonica* tadpoles was conservatively determined as 43 °C since tadpoles showed weak avoidance at 42 °C in [supplementary fig. S7B \(Supplementary Material](#) online), although they did not show significant avoidance in the same test temperature in D and E. (H) Typical traces of the $[Ca^{2+}]_i$ response to heat in DRG neurons from *B. japonica*. The upper and lower traces show changes in $[Ca^{2+}]_i$ and temperature, respectively. (I, J) Distributions (I) and average thermal activation thresholds (J) of heat-responsive DRG neurons from *B. japonica*, *B. buergeri*, and *Ra. japonica*. P -values < 0.05 are indicated (one-way ANOVA followed by post-hoc Tukey's HSD test). Among all DRG neurons observed, 12 of 47 (four individuals), 6 of 26 (four individuals), and 39 of 83 (three individuals) were heat-responsive in *B. japonica*, *B. buergeri*, and *Ra. japonica*, respectively. The average thermal activation thresholds of heat-responsive DRG neurons in *B. japonica*, *B. buergeri*, and *Ra. japonica* were $43.3 \text{ }^\circ\text{C} \pm 1.0$ ($n = 12$), $41.7 \text{ }^\circ\text{C} \pm 1.7$ ($n = 6$), and $36.9 \text{ }^\circ\text{C} \pm 0.6$ ($n = 39$), respectively.

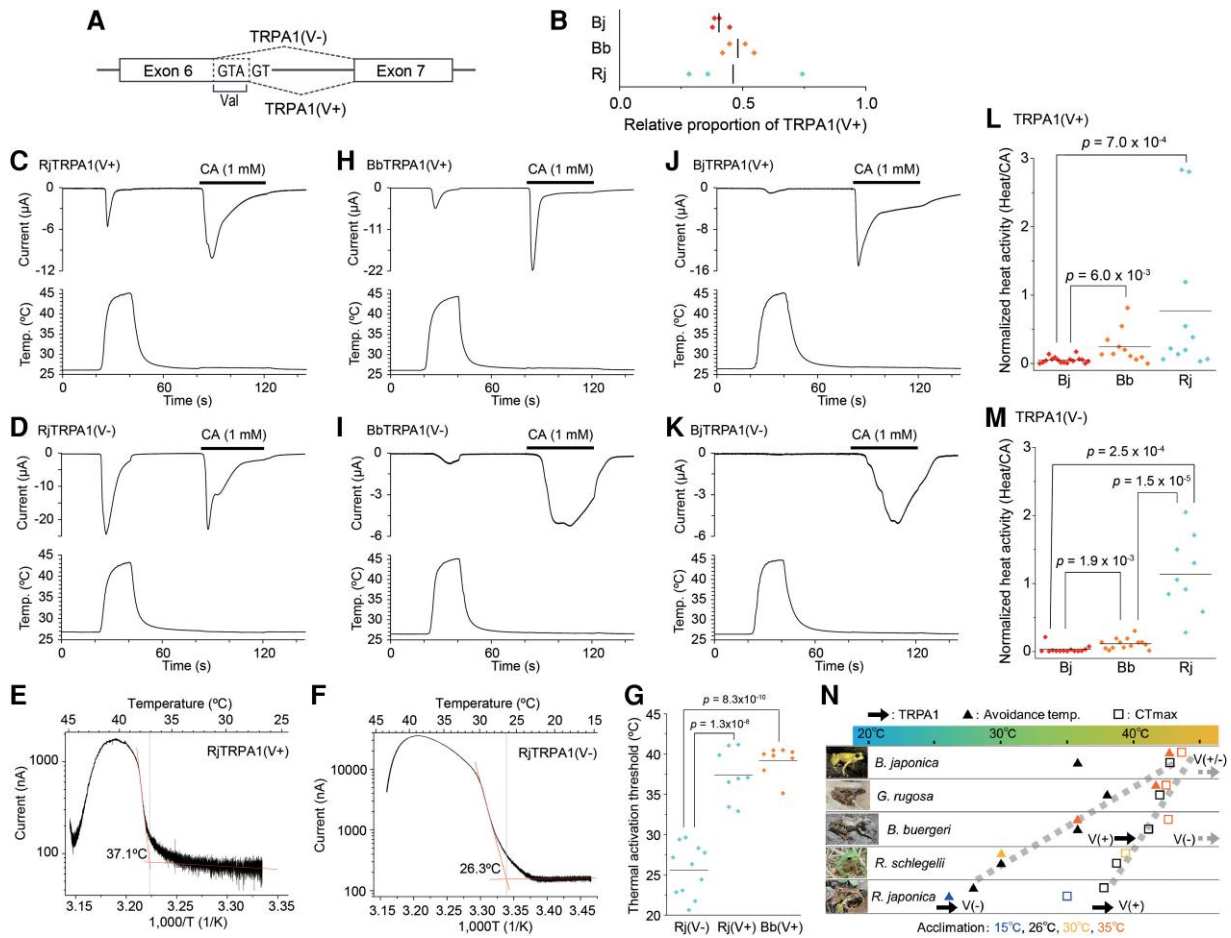


FIG. 3. Species-specific divergence of the thermal properties of TRPA1 AS variants among frogs. (A) The genomic structure of TRPA1 illustrating generation of a novel AS variant. (B) The relative proportion of TRPA1(V+) mRNA. The relative amounts of TRPA1(V+) and TRPA1(V−) were determined by direct sequencing of the TRPA1 DNA fragment amplified by RT-PCR from multiple individuals. The dots indicate the value from each individual and the bars represent average values. (C, D) Representative traces of the current and temperature produced by *Xenopus* oocytes expressing TRPA1(V+) and TRPA1(V−) of *Rana japonica*. (E, F) Arrhenius plots for the current responses to heat stimulation for TRPA1(V+) (E) and TRPA1(V−) (F) of *Ra. japonica*. (G) The apparent thermal activation thresholds of TRPA1 estimated by an Arrhenius plot. The average thermal thresholds for activation of *Ra. japonica* TRPA1(V+) and TRPA1(V−) were $37.4^{\circ}\text{C} \pm 1.2$ ($n = 8$) and $25.6^{\circ}\text{C} \pm 1.0$ ($n = 11$), respectively. The dots indicate the value for individual *Xenopus* oocyte expressing TRPA1. The bars represent average values. P -values < 0.05 are indicated (ANOVA followed by post-hoc unpaired t -test with Bonferroni correction). (H–K) Representative traces of the current and temperature produced by *Xenopus* oocytes expressing TRPA1(V+) or TRPA1(V−) of *Buergeria buergeri* (H, I) and *Buergeria japonica* (J, K). The apparent thermal activation thresholds of *B. buergeri* TRPA1(V+) estimated by an Arrhenius plot are shown in G (see [supplementary fig. 55C](#), [Supplementary Material](#) online). The average thermal threshold for activation of *B. buergeri* TRPA1(V+) was $39.2^{\circ}\text{C} \pm 1.8$ ($n = 8$). (L, M) A graph summarizing the normalized heat-evoked activity of TRPA1(V+) and TRPA1(V−) among three anuran species. The current amplitude for heat stimulation was normalized to CA stimulation in each oocyte to compensate for differences in expression efficiency. The dots indicate the value obtained from individual *Xenopus* oocytes expressing TRPA1. The bars represent average values. P -values < 0.05 are indicated (Kruskal–Wallis test followed by post-hoc Mann–Whitney U test with Bonferroni correction). (N) A summary of the CT_{max} , avoidance temperature, and thermal property of TRPA1 among anuran species. The thermal activation thresholds of TRPA1 for each species are shown with black arrows. Gray arrows depict an absence of heat-evoked activity below 45°C , which was the highest applicable temperature to *Xenopus* oocytes because endogenous heat-evoked currents were observed above this temperature.

Notably, the avoidance index of warm-acclimated *B. japonica* tadpoles was significantly lower than that of tadpoles reared at 26°C in either the 40°C or 42°C test condition (fig. 2E, [Supplementary movies 2 and 3](#), [Supplementary Material](#) online). In particular, the average avoidance index reached nearly 0 in the 40°C test chamber conditions, indicating that avoidance from this temperature was completely diminished after warm acclimation in *B. japonica* tadpoles (fig. 2E). In contrast, warm-acclimated *B. japonica* tadpoles escaped from the

44°C test chamber (fig. 2D), suggesting that tadpoles still maintained an avoidance response even after warm acclimation.

The acclimation effect was also examined in the other four species. In *G. rugosa* tadpoles, the avoidance temperature of which was relatively high, 35°C acclimation significantly decreased the avoidance index in the 40°C test chamber condition, and the avoidance temperature increased up to 42°C after warm acclimation (fig. 2D and E). In contrast, *B. buergeri* tadpoles acclimated at

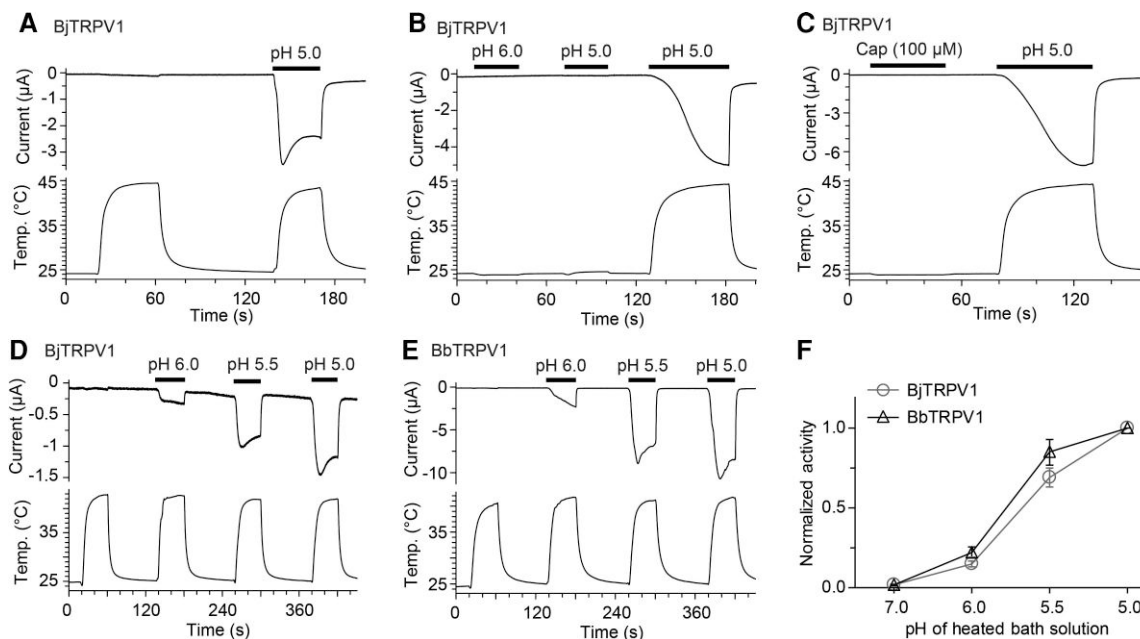


Fig. 4. Reduced heat activity of TRPV1 in two *Buergeria* species. Representative traces of the current and temperature obtained from *Xenopus* oocytes expressing TRPV1 from *Buergeria japonica* (A–D) or *Buergeria buergeri* (E). Solid bars indicate the duration of acid or capsaicin (Cap) stimulation. (F) Synergistic effect of heat and acid on *Buergeria* TRPV1. The amplitude of the current elicited by heat at varying pH values was normalized to that at pH 5.0 ($n=7$ for each).

35 °C exhibited only a slight reduction in the avoidance index, and no significant difference was observed between tadpoles reared at 26 °C versus 35 °C (fig. 2E). Similarly, in *Rh. schlegelii*, the avoidance index of tadpoles acclimated at 30 °C (the acclimation temperature was adjusted to the avoidance temperature of this species) was similar to that of the tadpoles reared at 26 °C (supplementary fig. S1C, Supplementary Material online). As shown in fig. 2D, *Ra. japonica* tadpoles reared at 26 °C avoided temperatures >28 °C. Considering that *Ra. japonica* tadpoles are normally reared at 15 °C, the tadpoles were likely to be in an acclimated physiological condition at 26 °C. To investigate the acclimation effect on *Ra. japonica*, the avoidance temperature was examined using tadpoles reared at 15 °C. Under this rearing condition, *Ra. japonica* tadpoles avoided temperatures >26 °C, suggesting that the acclimation effect was small in this species (supplementary fig. S1D, Supplementary Material online). Therefore, our results indicate that the effect of warm acclimation was prominent in the species with high avoidance temperatures, such as *B. japonica* and *G. rugosa* (fig. 2D and E).

Since the rearing temperature altered the avoidance temperatures in some of the species, we also examined the acclimation effect on CT_{max} to examine the precise relationship between avoidance temperature and heat tolerance among the five species. The CT_{max} was increased in warm-acclimated tadpoles in all examined species, but the effect was relatively small except for *Ra. japonica* tadpoles (0.6–1.6 °C, fig. 2F and supplementary fig. S2, Supplementary Material online). CT_{max} showed a relatively large shift (3.5 °C) in *Ra. japonica* tadpoles compared with other species. Finally, the correlation between

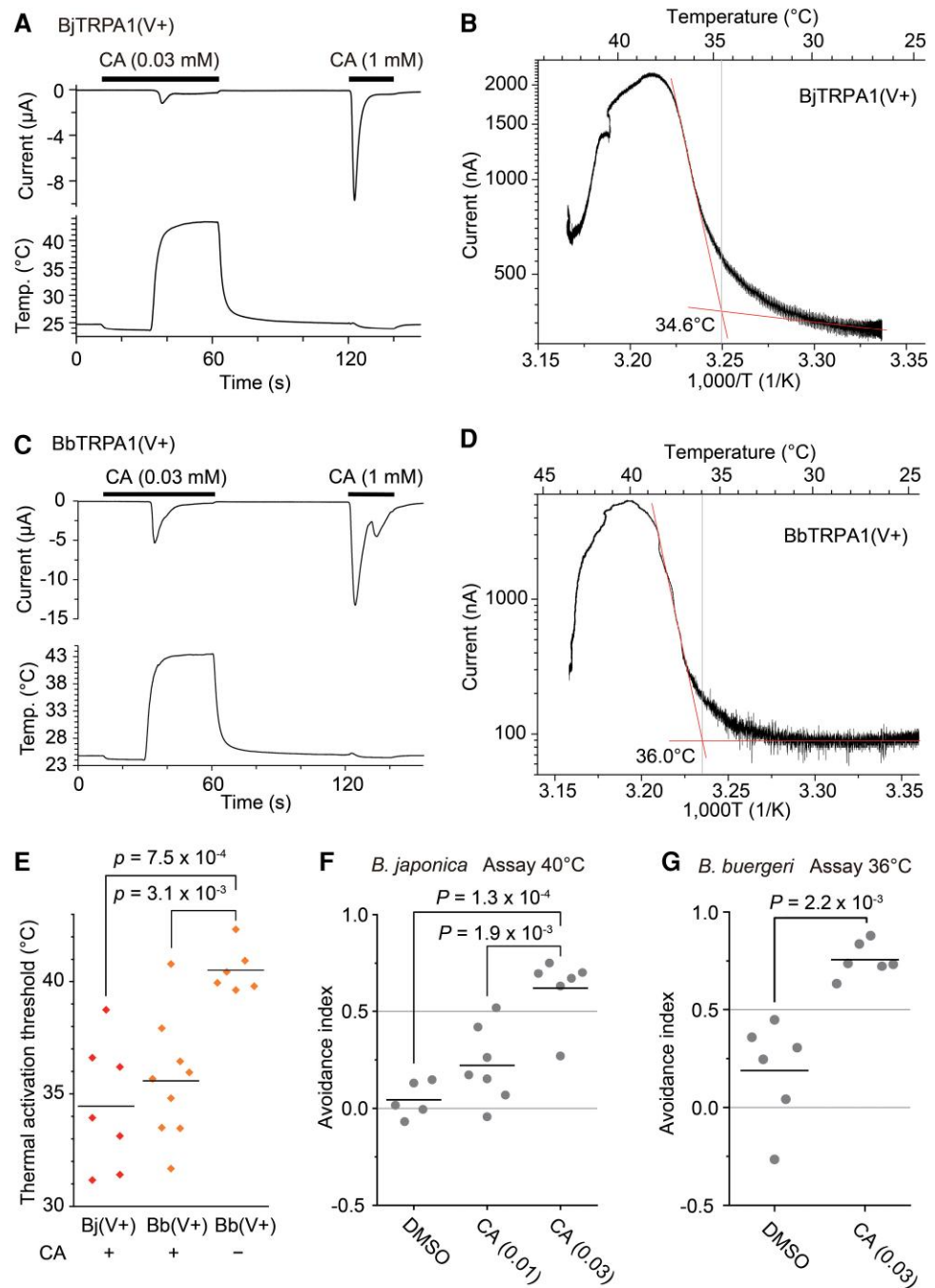
the avoidance temperature and CT_{max} was examined by taking the acclimation effect into consideration. A clear correlation was observed between avoidance temperature and CT_{max} (fig. 2G), suggesting that both factors are likely linked to the thermal niches of the five frog species. Notably, the species difference in the avoidance temperature was 2.6-fold higher than that in CT_{max} .

Next, to examine the relationship between avoidance behavior and sensory perception, we compared the thermal properties of primary sensory neurons among the frog species. Since sensory ganglia were difficult to identify in tadpoles, we dissected dorsal root ganglia (DRG) from froglets of *B. japonica*, *B. buergeri*, and *Ra. japonica*, the tadpoles of which showed the highest, intermediate, and lowest avoidance temperatures, respectively. Heat stimulation (~45 °C) was applied to DRG neurons, and changes in the intracellular calcium concentration ($[Ca^{2+}]_i$) were measured by calcium imaging experiments (fig. 2H). Among all of the observed DRG neurons, 25.5%, 23.0%, and 46.9% from *B. japonica*, *B. buergeri*, and *Ra. japonica* responded to heat stimulation, respectively. The average thermal activation threshold in DRG neurons gradually decreased from *B. japonica* to *Ra. japonica* (fig. 2I and J). These results suggest that the species difference in thermal sensitivity in primary sensory neurons was associated with that in the tadpole avoidance temperature.

Functional Changes in the Heat-Sensing TRPA1 Ion Channel among Frog Species

Avoidance behaviors are caused by the firing of nociceptive sensory neurons, which are triggered by the activation

Fig. 5. Stimulation with a TRPA1 agonist enhanced heat avoidance in anuran tadpoles. (A–D) Representative traces of current and temperature from *Xenopus* oocytes expressing TRPA1(V+) and Arrhenius plots of the currents evoked by combined stimulation with heat and 0.03 mM CA in *Buergeria japonica* (A and B) and *Buergeria buergeri* (C and D). (E) Comparison of the apparent thermal activation thresholds of *Buergeria* TRPA1 with versus without 0.03 mM CA. The average thermal thresholds for TRPA1(V+) activation in the presence of 0.03 mM CA were $34.5 \pm 1.1^\circ\text{C}$ ($n = 7$) and $35.6 \pm 0.9^\circ\text{C}$ ($n = 9$) for *B. japonica* and *B. buergeri*, respectively. The average thermal activation threshold of *B. buergeri* TRPA1(V+) under heat stimulation alone was $40.5 \pm 0.4^\circ\text{C}$ ($n = 6$) in the same preparations, demonstrating that stimulation with CA significantly increased the TRPA1 sensitivity to heat (ANOVA followed by post-hoc unpaired *t*-test with Bonferroni correction). (F and G) Enhanced heat avoidance in *Buergeria* tadpoles in the presence of CA. Water containing 0.01 mM CA, 0.03 mM CA, or DMSO (solvent) was used for the assay. The temperature in the test chamber was set to 40°C or 36°C for *B. japonica* (F) and *B. buergeri* (G), respectively. *Buergeria japonica* tadpoles were acclimated at 35°C for 1 day. The dots indicate the values obtained from individual tadpoles, and the bars represent the average values. *P*-values < 0.05 are indicated (ANOVA followed by post-hoc unpaired *t*-test with Bonferroni correction in F or Welch's *t*-test for G).



of heat-sensing ion channels such as TRPV1 and TRPA1 (Caterina et al. 1997, 2000; Viswanath et al. 2003; Rosenzweig et al. 2005; Saito et al. 2012, 2014, 2019). To investigate the association between heat avoidance behavior and these noxious heat sensors, we cloned TRPA1 from *B. japonica*, *B. buergeri*, and *Ra. japonica*. During the cloning process, we newly found a novel AS variant of TRPA1 from all three frog species. This AS variant is produced by alternative splicing at the 5' end of the intron between exons 6 and 7, which generates a single valine insertion in the canonical TRPA1 AS variant common among

vertebrate species (fig. 3A). This single valine insertion was located at the position 277 at the boundary between the sixth and seventh ankyrin repeat domains (in *B. japonica* and *B. buergeri* TRPA1, supplementary figs. S3 and S4, Supplementary Material online). The novel and canonical AS variants were named TRPA1(V+) and TRPA1(V–), respectively. The relative proportions of TRPA1(V+) mRNA ranged from 42% to 48% on average among three species, although a large variation was observed among individuals in *Ra. japonica* (fig. 3B and supplementary fig. S3D, Supplementary Material online). The proportion of amino

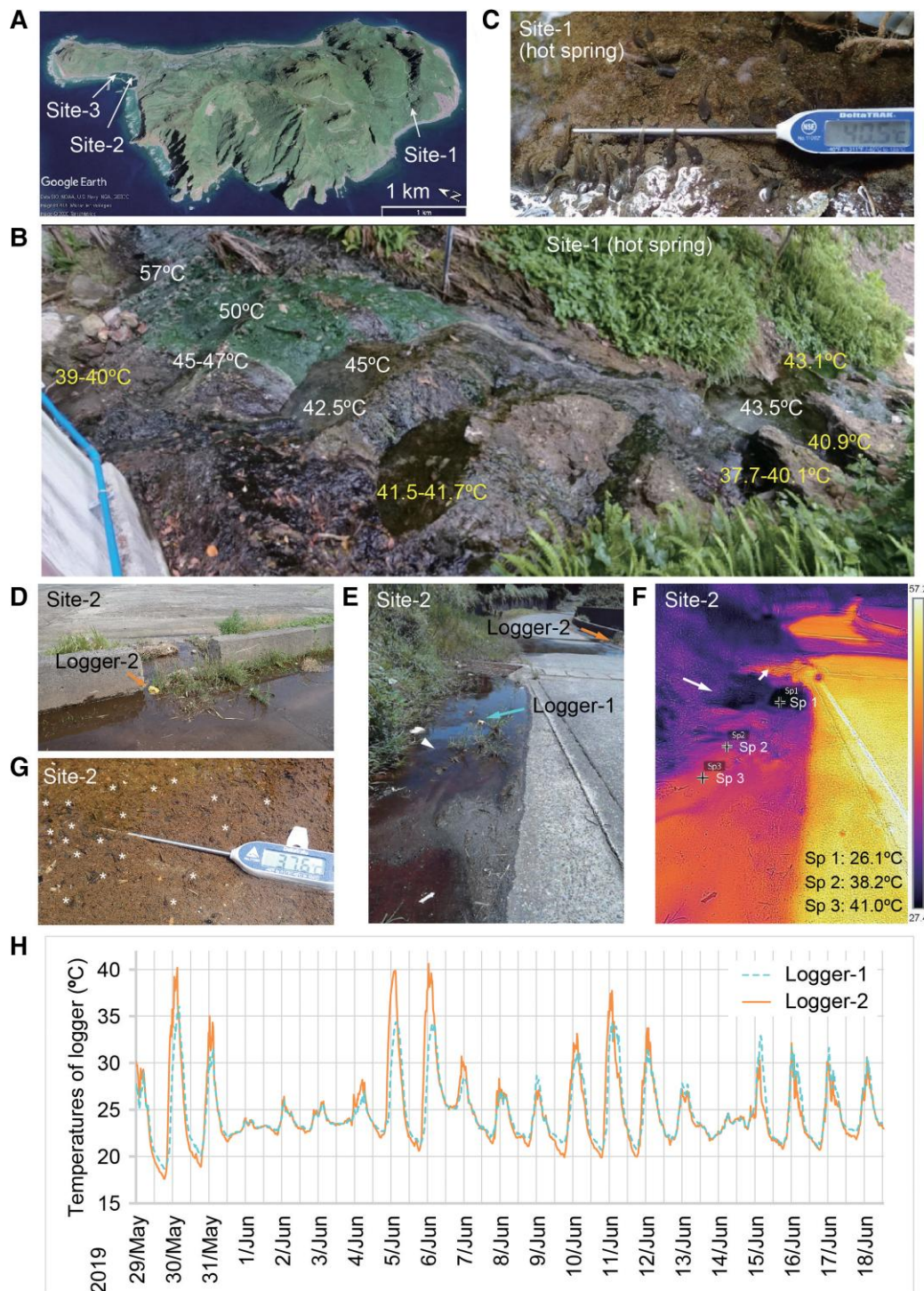


Fig. 6. Thermal fluctuations in the natural habitats of *Buergeria japonica* tadpoles. (A) A small volcanic island, Kuchinoshima. The image was obtained from Google maps. Arrows indicate the locations at which field observations were performed. (B) Variation in water temperatures in Seranma hot spring. Small pools with varying temperatures are connected in the stream. The water temperatures of the pools where multiple tadpoles were found are shown in yellow font. Field observations were conducted at 15:00–16:00 on May 27, 2017. (C) Many tadpoles were found in water with temperatures reaching 40 °C in Seranma hot spring. This image was taken at 16:20 on June 18, 2018 (See [supplementary movie 4, Supplementary Material](#) online). (D and E) Shallow puddles where tadpoles were found on Kuchinoshima Island (site 2 in A). Arrows indicate the locations of the temperature loggers placed in the puddles. (F) A thermal image of the puddle shown in E. This image was taken at 13:53 on May 30, 2019. The water was heated by solar radiation on a sunny day. Steep thermal gradients had formed due to cool water continuously flowing into the puddle (large white arrow) and draining into the ditch (small white arrow). (G) Tadpoles found in the puddle shown in E and F. This image was taken close to the location at which the logger 1 was placed (arrowhead in E) at 13:43 on May 30, 2019 (see [Supplementary movie 5, Supplementary Material](#) online). Tadpoles are marked with asterisks. (H) Water temperatures obtained by the temperature loggers shown in D and E. Temperatures were recorded from May 29 to June 18, 2019 (see [supplementary fig. S8, Supplementary Material](#) online).

acid differences in TRPA1(V−) was 4.9% between *B. japonica* and *B. buergeri*, 11.5% between *B. japonica* and *Ra. japonica*, and 11.5% between *B. buergeri* and *Ra. japonica*.

Next, the channel properties of TRPA1 were examined by expressing TRPA1 in the *Xenopus laevis* oocytes, and ionic currents were measured by an electrophysiological approach. Both AS variants of *Ra. japonica* TRPA1 responded to heat and cinnamaldehyde (CA), a well-known TRPA1 agonist (fig. 3C and D). The sensitivity to CA was higher for TRPA1(V+) than TRPA1(V−) (supplementary fig. S5A and B, Supplementary Material online). In addition, TRPA1 AS variants of *Ra. japonica* showed a difference in thermal sensitivity. Apparent thermal activation thresholds of TRPA1(V+) and TRPA1(V−) were 37.4 ± 1.1 °C ($n = 8$) and 25.6 ± 1.0 °C ($n = 11$), respectively (fig. 3E–G). These results indicate that a single valine insertion in the ankyrin repeat domains considerably alters both the chemical and thermal sensitivities of TRPA1.

Interestingly, the TRPA1 AS variants exhibited species-specific responses to heat. In *B. buergeri*, TRPA1(V+) apparently responded to heat stimulation, while TRPA1(V−) showed only a weak response to heat (fig. 3H and I). On the other hand, in *B. japonica*, the responses to heat stimulation by both TRPA1 AS variants were nearly abolished (fig. 3J and K). In both species, CA-evoked currents were observed in both TRPA1 AS variants, and the sensitivity of TRPA1(V+) was higher than that of TRPA1(V−), which was similar to the pattern seen in *Ra. japonica* TRPA1 (supplementary fig. S5A and S5B, Supplementary Material online). These results indicate that a single valine insertion altered the thermal properties of TRPA1 in a species-specific manner, while the effect of a valine insertion in TRPA1 sensitivity to chemical was similar among the species.

To examine the association between TRPA1 thermal properties and avoidance temperature, the normalized heat-evoked activities of TRPA1 were compared. The current amplitudes evoked by heat stimulation were normalized to the following CA-evoked currents to compensate for the expression efficiency among oocytes (fig. 3C, D, H–K). Since the TRPA1 sensitivity to CA differed between the two AS variants, normalized heat-evoked activity was compared separately. In both TRPA1 variants, the average normalized heat-evoked activity was highest and lowest in *Ra. japonica* and *B. japonica*, respectively, which was consistent with variation in avoidance temperature among the three species (fig. 3L and M). In addition, *Ra. japonica* possessed TRPA1 AS variants with higher (37.4 ± 1.1 °C) and lower (25.6 ± 1.0 °C) apparent thermal activation thresholds as mentioned above, while *B. buergeri* only possesses TRPA1(V+) with a higher threshold (39.2 ± 0.7 °C, $n = 8$, fig. 3G and supplementary fig. S5C, Supplementary Material online). Note, the thermal activation thresholds for TRPA1(V−) of *B. buergeri* and both AS variants of *B. japonica* could not be estimated due to the small current amplitudes elicited by heat stimulation. In summary, the species difference in TRPA1 thermal activity and sensitivity was associated with the difference in avoidance temperature among the species (fig. 3N).

The Lack of Heat-evoked Responses in Another Heat-sensing Ion Channel, TRPV1, in *Buergeria* Species

TRPA1 heat-evoked activity was nearly abolished in *B. japonica*, the avoidance temperatures of which reached as high as 44 °C (fig. 2D). In addition to TRPA1, TRPV1 also serves as a noxious heat sensor, and we previously showed that several clawed frog species possess a TRPV1 molecule activated by temperatures around 40 °C (Ohkita et al. 2012; Saito et al. 2016, 2019), which prompted us to also examine the properties of the TRPV1 channel. TRPV1 was cloned from *B. japonica*, and its properties were examined by expressing it in *Xenopus* oocytes. As expected, *B. japonica* TRPV1 did not show any response to heat stimulation alone. In addition, stimulation with acid or capsaicin, a TRPV1 agonist, did not elicit any response (fig. 4A–C). However, TRPV1 elicited apparent currents in response to combined stimulation with heat and acid. These results suggest that *B. japonica* TRPV1 has lost the ability to respond to heat, acid, or capsaicin, but it has maintained proper channel structure for its function.

To examine whether the loss of heat-evoked activity of TRPV1 occurred specifically in *B. japonica*, TRPV1 was also cloned from the closely related congeneric species *B. buergeri*. The proportion of amino acid differences in TRPV1 between the two *Buergeria* species was 4.8%. *Buergeria buergeri* TRPV1 showed similar properties to those of *B. japonica* TRPV1. It was not activated by heat alone, while combined stimulation with heat and acid evoked a clear response (fig. 4D and E). The heat-evoked currents of TRPV1 increased gradually by lowering the pH of the bath solution, with a similar degree of change between *B. japonica* and *B. buergeri* (fig. 4F). It is worth mentioning that the current amplitude of TRPV1 tended to be larger in *B. buergeri* than *B. japonica*. In brief, the TRPV1 heat response was absent in *B. japonica*, despite similar channel properties of TRPV1 as those of the congeneric species *B. buergeri*.

The alignment of TRPV1 with those of other vertebrate orthologs revealed that amino acids differed in BjTRPV1 in two sites that are known to be involved in capsaicin binding in rat TRPV1 (Jordt and Julius 2002; Gavva et al. 2004; Ohkita et al. 2012; Saito et al. 2016; Y511 and T550, supplementary fig. S6, Supplementary Material online). These amino acid substitutions potentially related to the loss of TRPV1 sensitivity to capsaicin in *B. japonica*. On the other hand, several amino acids residues, which are involved in the TRPV1 activation by acidic stimulation in rat TRPV1 (Jordt et al. 2000; Ryu et al. 2007), were conserved in BjTRPV1 except for K535 (supplementary fig. S6, Supplementary Material online). E600, involved in the synergistic effect between acid and heat in rat TRPV1, was conserved in TRPV1 from two *Buergeria* species.

Involvement of TRPA1 and TRPV1 in Heat Avoidance by Tadpoles

Comparison of TRPA1 among three frog species supported our hypothesis that the species differences in TRPA1

activity and sensitivity to heat are related to the tadpole avoidance behaviors of each species. However, the contribution of TRPA1 to heat avoidance behaviors in amphibian tadpoles remains elusive. Previous studies showed synergism between the thermal and agonistic responses of TRPA1 (Kurganov et al. 2014); thus, involvement of TRPA1 in avoidance behaviors can be examined by using a pharmacological approach. To this end, we first examined the synergism between heat and an agonist (CA) in *Xenopus* oocytes expressing TRPA1. Under the threshold concentration of CA (0.03 mM), *B. japonica* TRPA1(V+) elicited apparent heat-evoked currents with an average thermal activation threshold of 34.5 ± 1.1 °C, $n = 7$ (fig. 5A and B). In addition, the apparent thermal activation threshold of *B. buergeri* TRPA1 decreased by approximately 5 °C under 0.03 mM CA (without CA: 40.5 ± 0.4 °C, $n = 6$; with CA 35.6 ± 0.9 °C, $n = 9$; fig. 5C–E).

Next, heat avoidance by tadpoles was examined by adding lower concentrations of CA to water in the two-chamber choice assay. Addition of CA increased the avoidance index in a dose-dependent manner, and the avoidance index was significantly higher for 0.03 mM CA than for 0.01 mM CA or solvent (dimethyl sulfoxide, DMSO) in *B. japonica* tadpoles acclimated to 35 °C (fig. 5F). In addition, tadpoles of *B. buergeri* and *Ra. japonica* also displayed a significantly higher avoidance index in the presence of low CA concentrations compared with the solvent control (fig. 5G and supplementary fig. S7A, Supplementary Material online). These results suggest that stimulation of anuran tadpoles with lower concentrations of CA resulted in sensitization of TRPA1 and increased avoidance behaviors.

In addition to TRPA1, we also observed a synergistic effect between acidic and thermal stimulations on TRPV1, as shown in fig. 4; thus, we also examined the heat avoidance behaviors of tadpoles by changing the water pH used for the assay. As a result, lowering the water pH significantly increased the avoidance index of tadpoles in both *B. japonica* and *B. buergeri* (supplementary fig. S7B and C, Supplementary Material online).

Buergeria japonica Tadpoles Experience Large Temperature Fluctuations in their Natural Habitat

To gain insight into the ecological significance of reduced heat avoidance in *B. japonica* tadpoles, field observations were conducted on Kuchinoshima Island. In Seranma hot spring (fig. 6A, site 1), tadpoles are found in a shallow stream fed by several hot springs. As shown in fig. 6B, the stream is formed from small pools with variable temperatures. In our observations, multiple tadpoles were found in pools with temperatures as high as 43 °C, as reported previously (Komaki, Lau, et al. 2016; fig. 6B and 6C and Supplementary movie 4, Supplementary Material online).

Tadpoles of *B. japonica* can generally be found in various aquatic habitats such as small streams, artificial ditches, and shallow puddles (Wu and Kam 2005; Tominaga et al. 2015; Komaki, Igawa, et al. 2016; Komaki, Lau, et al. 2016; Komaki et al. 2020). Since water in shallow puddles with open

environments can be heated upon exposure to sunlight, we monitored temperature fluctuations in such habitats by placing temperature loggers (sites 2 and 3 in fig. 6A, D, E and supplementary fig. S8, Supplementary Material online). As expected, water temperatures fluctuated daily in the shallow pools, reaching as high as 40 °C on sunny days (fig. 6H and supplementary fig. S8E, Supplementary Material online). The maximum daily temperature variation during our observations was from 17.6 °C to 40.2 °C (from 5:20 to 14:00 on May, 30 2019; fig. 6H, logger 2). In addition, extreme thermal gradients had formed in heated puddles due to a continuous flow of cool water into them (fig. 6F supplementary fig. S8B, Supplementary Material online). Even under such conditions, *B. japonica* tadpoles were found in areas where temperatures reached approximately 38 °C, although cooler areas existed in the same puddle (fig. 6E–G, supplementary fig. S8C and supplementary movie 5, Supplementary Material online). In summary, our field observations revealed that *B. japonica* tadpoles were occasionally exposed to high temperatures across a wide range of its natural habitat.

Thermal Experience of Tadpoles Varied among Species in their Natural Habitats

To compare the thermal experience of tadpoles among frog species in the wild, we also monitored the temperatures at the collection sites of *B. buergeri*, *Rh. schlegelii*, and *Ra. japonica*. *Buergeria buergeri* spawns eggs in relatively cool mountain streams (Fukuyama and Kusano 1992). Tadpoles were found at the stream margin covered with stones (supplementary fig. S9A–D, Supplementary Material online). Water temperatures reached nearly 30 °C at the stream margin on a sunny day in the summer. Under such conditions, tadpoles stayed at the stream margins even though the temperatures near midstream were relatively stable during the day (supplementary fig. S9D and E, Supplementary Material online). Therefore, *B. buergeri* tadpoles experience temperature fluctuations and are occasionally exposed to warm temperatures even though they inhabit cool mountain streams.

On the other hand, *Ra. japonica* and *Rh. schlegelii* spawn eggs in rice fields, marshes, and shallow puddles and frequently share the same habitats. However, the breeding seasons of the two species differ. *Rana japonica* spawns eggs in late winter, while *Rh. schlegelii* spawns eggs in spring. We performed field observations in the habitats shared by both species (supplementary fig. S9F, Supplementary Material online). In our observations, *Ra. japonica* spawned eggs from late January to early March, and tadpoles developed from March to June under cool thermal conditions. *Rana japonica* tadpoles reached the metamorphic stage in late May, and most tadpoles completed metamorphosis in late June, when the daily maximum water temperatures were mostly below 25 °C (supplementary fig. S9G–I, Supplementary material online). Metamorphosis of *Rh. schlegelii* tadpoles began in late June and completed in early August, when the daily maximum water temperature was frequently at or close to

25 °C. In summary, our field observations revealed that the thermal experiences of tadpoles are highly different among frog species due to variation in breeding seasons and the water environments used for spawning.

Discussion

The Relationships Between Heat Avoidance and Tolerance among Frog Species Inhabiting Different Thermal Niches

We compared the heat tolerance (CT_{max}) and avoidance temperatures of tadpoles among five frog species occupying different microhabitats and found that both factors are highly correlated with each other (fig. 2G). The order of the values among species was consistent with our field observations in the natural habitats of each species. For example, *Ra. japonica* tadpoles, which exhibited the lowest CT_{max} and avoidance temperature, grow in spring and complete metamorphosis before early summer, when water temperatures are generally below 25 °C (supplementary fig. S9H and I, Supplementary Material online). In contrast, *B. japonica* tadpoles, which exhibited the highest CT_{max} and the avoidance temperature, were occasionally exposed to temperatures near 40 °C on sunny days in summer (fig. 6 and supplementary fig. S8, Supplementary Material online). *Buergeria buergeri* tadpoles, which had CT_{max} and avoidance temperatures ranking intermediate among the species, were exposed to warm temperatures at the stream margin even though they inhabit cool mountain streams (supplementary fig. S9A–E, Supplementary Material online). These results indicate that heat tolerance and avoidance temperatures are associated with the habitat thermal conditions of each frog species.

Previous studies showed that the variation in CT_{max} is weakly correlated with realized thermal niches among a wide variety of species (Sunday et al. 2011, 2012; Araujo et al. 2013). We also observed that the range in the CT_{max} was relatively narrow, and even cool-adapted species showed high CT_{max} values. In contrast, avoidance temperatures showed a large variation, and the species difference in avoidance temperatures was 2.6 times larger than that in the CT_{max} values (fig. 2G). These results strongly indicate that avoidance behaviors changed flexibly during the evolutionary processes compared with the heat tolerance of the species. The differences between the CT_{max} and avoidance temperature of each species increased as these values decreased, and there was a large difference between the two parameters in cool-adapted species such as *Ra. japonica* and *Rh. schlegelii* (fig. 3N). In such species, avoidance temperatures might be much lower than CT_{max} to allow their safe escape from potentially harmful temperatures. Alternatively, CT_{max} is maintained at a higher level to survive a heat wave, although these species might have a lower chance of being exposed to such a climatic event. In contrast, avoidance temperatures were fine-tuned and maintained just below the CT_{max} in warm-adapted species such as *B. japonica* and *G. rugosa*. Interestingly, we observed a large change in the avoidance temperature by increasing

rearing temperatures in these two species (fig. 2D and 2E). In contrast, the acclimation effect was not clearly observed in *B. buergeri*, which is closely related to *B. japonica*. Our field observations in the habitats of *B. japonica* showed that tadpoles are exposed to warm temperatures before challenged by extreme heat (fig. 6 and supplementary fig. S8, Supplementary Material online). All of these results suggest that this feature has evolved in warm-adapted species to allow adaptation to habitats with large temperature fluctuations.

Ecological Implications for Reduced Thermal Perception in *Buergeria japonica*

We emphasize the importance of thermal avoidance, rather than preference, in determining fundamental thermal niches, since avoidance temperatures define the acceptable thermal range of a species. For example, *B. japonica* tadpoles from Taiwan were reported to prefer temperatures around 24–30 °C in a laboratory thermal gradient assay (Wu and Kam 2005). In addition, field observations from a Kuchinoshima hot spring revealed that tadpoles prefer temperatures lower than 40 °C (Komaki et al. 2020). While thermal preference helps identify suitable temperature ranges, avoidance temperatures determine the acceptable thermal ranges under harsh thermal conditions. Tadpoles must survive in the restricted aquatic environments selected by the parental frogs; these water temperatures fluctuate, and tadpoles can be exposed to heat under certain conditions. *Buergeria japonica* tadpoles avoided high temperature when reared under preferable thermal conditions (26 °C), while their avoidance temperature increased near CT_{max} after experiencing warmth. However, even after acclimation, tadpoles still maintained their avoidance to 44 °C, just below their CT_{max} . Increased avoidance temperatures in *B. japonica* tadpoles allowed them to fully capitalize on their thermal tolerance, which may enable tadpoles to explore a wider habitat range under extreme thermal events.

Molecular Basis for the Evolutionary Shift in Tadpole Heat Avoidance

We showed that the species difference in the thermal sensitivity of DRG neurons was consistent with the avoidance temperatures of tadpoles among three frog species (fig. 2I and 2J), which supports our idea that noxious heat perception changed with the ecological niches of species during evolution. To demonstrate the involvement of TRPA1 in tadpole heat avoidance behaviors, we took advantage of the synergistic response of TRPA1 to heat and chemical stimulation. We first showed that stimulation with a low concentration of CA decreased the apparent thermal activation threshold of TRPA1 in a heterologous expression system and then further showed that administration of lower concentrations of CA to tadpoles significantly increased the avoidance index of all three anuran species examined at their respective test temperatures (fig. 5). This suggests that TRPA1 was sensitized by weak non-thermal

stimulation, thereby strengthening the heat avoidance behavior of tadpoles. Therefore, our results strongly indicate that TRPA1 is involved in heat avoidance behavior in anuran tadpoles.

We identified a novel TRPA1 AS variant that is identical to the canonical AS variant except with a single valine insertion between the ankyrin repeat domains. Interestingly, the single valine insertion within TRPA1 considerably altered its heat response in a species-specific manner. The heat-evoked activity of both TRPA1(V+) and TRPA1(V-) was nearly absent in *B. japonica*, where as in *B. buergeri* TRPA1(V+) retained moderate heat-evoked activity. In contrast, both AS variants possessed an apparent response to heat in *Ra. japonica* (fig. 3). The normalized heat-evoked activity of TRPA1 decreased in the order of *Ra. japonica* > *B. buergeri* > *B. japonica* (fig. 3L and M), which was the reverse order for tadpole avoidance temperatures (fig. 2D). In the case of TRPA1(V-), the concentration of CA (1 mM) used for normalization of heat-evoked currents was suboptimal in BjTRPA1(V-) and BbTRPA1(V-) since 1 mM was lower than saturating concentrations, while BjTRPA1(V-) showed nearly full activation at 1 mM of CA (supplementary fig. S5A, Supplementary Material online). This may lead to an overestimation of the normalized heat-evoked activity in BjTRPA1(V-)/BbTRPA1(V-) compared with that in RjTRPA1(V-). However, even under such conditions, normalized heat-evoked activity of RjTRPA1(V-) was significantly higher than BjTRPA1(V-) and BbTRPA1(V-). In addition, *Ra. japonica* possessed TRPA1(V-) with considerably higher thermal sensitivity (fig. 3C). All of these results suggest that the evolutionary shift in the TRPA1 thermal response led to the divergence in heat avoidance behavior among frog species adapted to diverse thermal niches.

The near disappearance of the heat-evoked activity of TRPA1(V-) likely occurred at the latest in the most recent common ancestor of the two *Buergeria* species, since TRPA1(V-) possesses obvious heat sensitivity in several clawed frog species and *Ra. japonica*, as well as other vertebrates (Saito et al. 2012, 2016, 2019; Kurganov et al. 2014). Subsequently, the heat-evoked activity of TRPA1(V+) was also abolished in *B. japonica*. On the other hand, the sensitivity of TRPA1(V+) to CA was higher than that of TRPA1(V-) in all three species examined (supplementary fig. S5A and B, Supplementary Material online). Therefore, the thermal activity of TRPA1 AS variants had been altered independently in a species-specific manner, while both AS variants have maintained their sensitivity to a chemical agonist during evolution. Our comparative analysis revealed a unique evolutionary trajectory of TRPA1 functional properties during the adaptation to diverse thermal niches among anurans.

It is intriguing to investigate the origin and evolutionary processes of TRPA1(V+). TRPA1(V+) is found in species belonging to genus *Rana* and *Buergeria* which diverged approximately 85 million years ago (Kumar et al. 2017). Furthermore, TRPA1(V+) was not identified in our previous studies focusing on lizards and chickens (Saito et al.

2012, 2014), thus TRPA1(V+) might have emerged in amphibian lineages. Future investigations using diverse amphibian species will clarify the origin and functional evolution of TRPA1 AS variants. On the other hand, the relative proportions of two TRPA1 AS variants highly varied among individuals in *Ra. japonica* (fig. 3B). Changes in their expression potentially alter the thermal perception at neural and individual levels since thermal sensitivity differed between TRPA1 AS variants in this species. Currently, we do not know whether the expression of TRPA1 AS variants is regulated under specific physiological conditions, and further investigations are required to understand their physiological and adaptive roles.

Functional differentiation of frog TRPA1 AS variants illuminates the importance of the N-terminal portion of the ankyrin repeat domains in the thermal and chemical sensitivities of TRPA1. A previous random mutagenesis study on mouse TRPA1 showed that three single-mutations within the sixth ankyrin repeat domain affect the thermal sensitivity of this ion channel (Jabba et al. 2014). TRPA1 is characterized by the long stretch of ankyrin repeat domains in the N-terminal region, and our results showed that a slight structural change in these regions extensively altered the thermal response of TRPA1. Although the cryoelectron microscopic structure of human TRPA1 has been resolved, a large portion of the ankyrin repeat domains is lacking due to lower resolution in the N-terminal region (Paulsen et al. 2015). Thus, the structural roles of the N-terminal region in the thermal and chemical activities of TRPA1 remain elusive. The alignment of TRPA1 among three frog species examined in the present study identified 165 variable sites in the entire TRPA1 sequences (supplementary fig. S4, Supplementary Material online). The accumulation of amino acid substitutions in each species resulted in the difference in the epistatic interaction between unidentified amino acids and a single valine inserted in TRPA1(V+), which cause their functional diversifications among species. Comparative analysis of AS TRPA1 variants among frogs will facilitate our understanding of the structural basis of the thermal and chemical activation of TRPA1 in the future.

It has been reported that several TRP channels are involved in noxious heat detection in mice (Vandewauw et al. 2018). Thus, we examined the channel properties of TRPV1 in *B. japonica*, the tadpoles of which exhibit reduced heat avoidance, and found that the heat-evoked activity of TRPV1 is also absent in *B. japonica* (fig. 4A and D). Additionally, *B. buergeri* TRPV1 showed almost no response to heat (fig. 4E). We previously showed that TRPV1 from several clawed frog species exhibit clear heat responses (Ohkita et al. 2012; Saito et al. 2016, 2019), suggesting that the reduction in TRPV1 thermal activity likely occurred at latest in the common ancestor of the two *Buergeria* species and preceded the reduction in heat avoidance behavior in the *B. japonica* lineage. Further investigations using additional anuran species will help reveal the detailed evolutionary process of TRPV1 in term of thermal adaptation.

It is worth noting that the role of TRPV1 as a functional channel has been maintained considering that it was activated by combined stimulation with heat and acid (fig. 4D–F). Furthermore, the tadpoles of two *Buergeria* species showed enhanced avoidance behavior in response to heat upon acidification of the water in the two-chamber choice assay (supplementary fig. S7B and C, Supplementary Material online). The synergism between heat and acid on TRPV1 is well known in mammals (Tominaga et al. 1998; Julius 2013). TRPV1 is sensitized upon inflammation due to the acidification in injured tissues, leading to the activation of TRPV1 under normal body temperatures in mammals. It is possible that TRPV1 is sensitized under injured conditions in anuran tadpoles and helps them to avoid unfavorable heat in unhealthy physiological conditions. In addition, tadpoles are sometimes exposed to acidic environments in their habitats. The pH of the water in a pool at site 3 was slightly acidic (pH ~6) although the water in Seranma hot spring was neutral (approximately pH 7, data not shown). These observations suggest that TRPV1 has retained its function as a potential heat sensor to escape hazardous environmental stimuli under specific circumstances.

Conclusion

The thermal properties of TRPA1 or TRPV1 were recently reported to vary across closely related species of mammals, clawed frogs and anole lizards inhabiting different thermal niches (Laursen et al. 2015, 2016; Saito et al. 2016, 2019; Saito and Tominaga 2017; Akashi et al. 2018). Specially, the heat sensitivity of TRPV1 in camels, which possess heat tolerance, was found to be nearly absent (Laursen et al. 2016); this resembles the situation observed in *B. japonica* in the present study. Thermal perception of noxious heat can define the fundamental niche of a species, thereby potentially influencing species distribution. Our findings emphasize the importance of considering evolutionary changes in thermal perception and avoidance behaviors for elucidating the mechanisms of thermal adaptation and the effect of global warming on species in the future.

Materials and Methods

Animal Samples

Buergeria japonica was collected from Seranma hot spring, Kuchinoshima, Kagoshima, Japan on April 30 and June 16, 2018 and May 29 and 30, 2019. Early-stage tadpoles (10–20 mm in size, Gosner stages 23–26) were generally collected (Gosner 1960). In some cases, mature adult frogs were collected, and fertilized eggs were obtained by pairing male and female frogs. Early-stage tadpoles were collected at Aikawa River in Hamamatsu, Shizuoka, Japan on July 23, 2017, July 14 and July 27, 2018, and July 13, 2019 for *B. buergeri*, and on August 10, 2020 and September 29, 2021 for *G. rugosa*, *Ra. japonica*, and *Rh. schlegelii* were collected at Okazaki, Aichi, Japan. *Rhacophorus schlegelii* tadpoles were collected on June 30 and July 16, 2018; May 18,

2019; and June 5, June 20, and July 3, 2021. Egg clutches of *Ra. japonica* were collected on Feb. 2 and Feb. 11, 2020 and Mar. 14, 2021. *Rana japonica* tadpoles developed from eggs were used for behavioral assays. Tadpoles were reared at approximately 26 °C (25–27 °C) on a 12 h:12 h light/dark cycle, except for *Ra. japonica* tadpoles, which were kept at 15 °C. Tadpoles were kept in a plastic container (in approximately 1 or 2 l water) and fed artificial food pellets ad libitum. Water was exchanged typically two or three times per week. Tap water was purified using a charcoal filter and used for rearing tadpoles and in the behavioral assays. Embryos or tadpoles were maintained under the above conditions for 4–111 days. Tadpoles used for behavioral experiments were at Gosner stages from 26 to 41. Acclimation temperatures were changed according to the avoidance temperatures of tadpoles in each species. For acclimation at 30 °C for *Rh. schlegelii* or 35 °C for *B. japonica*, *B. buergeri*, and *G. rugosa*, tadpoles (typically five individuals) reared at 26 °C were transferred to a plastic container (approximately 1 l) with an aquarium heater, and water was circulated by aeration. Tadpoles were maintained for 1 day (18–24 h) under these conditions and then used for the behavioral assays. For control experiments, tadpoles were reared under the same conditions without a heater and maintained for 1 day at 26 °C. Behavioral assays for tadpoles reared at 26 °C and those exposed to the acclimation temperatures were performed on the same day. *Rana japonica* tadpoles were acclimated at 26 °C for 6–19 days before the behavioral assays, since they were generally reared at 15 °C. Behavioral assays were performed during the light period from 13:00 to 20:30. Naïve tadpoles were used in most assays, but in a few assays, the same tadpoles were used two or three times due to a shortage of tadpoles. Froglets of *B. japonica*, *B. buergeri*, and *Ra. japonica* raised from tadpoles were used to dissect DRG. Froglets were maintained at room temperature (25–28 °C) and fed cricket larvae or aphids. For electrophysiological experiments, mature *X. laevis* females were purchased from Hamamatsu Seibutsu Kyouzai (Hamamatsu, Shizuoka, Japan) and reared at approximately 18 °C on a 14 h/10 h light/dark cycle.

All procedures involving the care and use of animals were approved by the committees for animal experimentation of the National Institute for Physiological Sciences (Okazaki, Aichi, Japan). Field research and sample collection of *B. japonica* on Kuchinoshima Island were approved by the mayor of Toshima village. *Buergeria japonica* populations from Taiwan and southern Ryukyu were recently reclassified as a new species (Wang et al. 2017; Matsui and Tominaga 2020); however, we consistently use *B. japonica* when citing previous findings regarding the Taiwanese populations in this manuscript to avoid confusion.

Field Observations

Field observations for *B. japonica* were conducted in Kuchinoshima, Kagoshima, Japan on May 27–31, 2017, June 14–19, 2018, and May 28–31, 2019. We observed tadpoles

in Seranma hot spring (site 1, [fig. 6](#)) and in shallow puddles near the harbor (sites 2 and 3, [fig. 6](#)), and water temperatures were measured periodically using a thermometer (Model 11062, DeltaTRAK, Pleasanton, CA, USA). Temperature loggers (KT-165F; Fujita Electric Works, Ninomiya, Kanagawa, Japan) were placed into shallow puddles at sites 2 and 3. The temperature logger was enclosed in a plastic bag and completely immersed in the water. We confirmed accurate measurement of the water temperatures by the loggers by manually measuring water temperatures at a nearby position using a thermometer on sunny days. Thermal images were taken using a the FLIRONE PRO thermal camera (FLIR Systems, Wilsonville, OR, USA) and analyzed using FLIR Tools v6.4 (FLIR Systems). The pH of the water was roughly measured using Tritest pH 1–11 pH test paper (Macherey-Nagel, Duren, Germany). Field observations of *B. buergeri* were also performed at the collection site at Aikawa River in Hamamatsu, Shizuoka, Japan ([supplementary fig. S9, Supplementary Material](#) online) on July 15 and July 27, 2018. Temperature loggers (KT-165F) were placed at the margin and near midstream. The field observations for *Ra. japonica* and *Rh. schlegelii* were conducted in a shallow pool (a small reservoir) situated beside the rice fields and mountains in Okazaki, Aichi, Japan. Temperature loggers (KT-165F) were placed in water and on the ground. The temperature logger on the ground was placed just beside the pool and was covered by a plant pod to minimize the effect of solar radiation. The field observations were conducted from late winter to midsummer. We visited the pool on different occasions and observed the approximate timings of spawning, hatching, and metamorphosis. Tadpoles were collected every 1–3 weeks, and their developmental stages were examined ([supplementary fig. S9G, Supplementary Material](#) online). We assumed that metamorphosis of the tadpoles was completed when almost all collected tadpoles exceeded stage 42 ([Gosner 1960](#)) in which the forelimb appeared.

Behavioral Assays

We set up a new assay for observing the behavioral response of tadpoles to a temperature ramp and determined the CT_{max} defined as the temperature at which tadpoles lose their righting reflex. Two aquarium heaters (200 W; Nisso, Higashiosaka, Japan) were placed on the bottom of a container, which was filled with water ([fig. 1A](#)). Then, an oval-shaped plastic chamber (long-axis length: 15.8 mm; short-axis length: 9.6 mm) containing 120 ml water (approximately 1.1 cm in depth) was placed on the heaters. A single tadpole was released into the chamber and then habituated for approximately 5 min. The tadpole was video recorded from above. Two thermal probes were placed on the wall of the chamber, and the temperature was recorded (once per second) using the TM-947SD thermometer (Lutron Electronic Enterprise, Taipei, Taiwan) during the assay. At the beginning of the assay, the water temperature was kept at around 26 °C for 2.5 min to monitor the basal swimming behaviors of the

tadpole, and water temperature was subsequently increased by approximately 3 °C/min. Water in the lower container was circulated using a pump to reduce temperature heterogeneity. In this way, ramp heating can be applied to a tadpole without any circulation in the chamber, which may affect swimming behavior. When a tadpole began to exhibit abnormal swimming behavior, it was immediately taken out of the chamber and allowed to recover at room temperature. Water in the chamber was replaced after every assay to minimize the effect of the previous assay. Tadpole movement was tracked using idTracker videotracking software ([Perez-Escudero et al. 2014](#)), and the swimming speeds of the tadpoles (cm/s) were calculated. The temperature at which the tadpole started to lose balance and exhibit abnormal swimming behavior, typically swimming sideways or upside down, was defined as the CT_{max} . The swimming speeds of the tadpoles obtained in each assay were plotted relative to the time to reach CT_{max} ([fig. 1](#) and [supplementary fig. S2, Supplementary Material](#) online). If tadpoles continuously stopped moving for more than approximately 1 min during the assay, the entire data set was omitted from the analysis.

The setup for the two-chamber choice assay was newly developed ([fig. 2A](#)). The assay chamber was constructed by connecting two circular plastic containers with a narrow path and filling it with 150 ml water (approximately 1.2 cm depth). The assay chamber was submerged in a container that was separated by a wall down the middle, and each compartment of the container was filled with water. A thermal difference in the assay chamber was formed by setting different water temperatures in each compartment of the lower container. A single thermal probe was placed at each end of the assay chamber and monitored using the TM-947SD thermometer during the assay. A single tadpole was released into the middle of the assay chamber, and its movement was tracked once it began to swim. The procedure for releasing a tadpole was slightly modified in the later assay. In the new procedure, a tadpole was released in the middle path, which was partitioned by a plastic wall, and habituated for 2–3 min. After the onset of video-recording from above, the partition was removed, which allowed the tadpoles to explore the entire assay chamber. Water in the assay chamber was replaced after every assay to minimize the effect of the previous assay.

The movement of a tadpole was tracked using the ANY-maze video tracking system (Stoelting, Wood Dale, IL, USA) and the time spent on each side of the chamber and the middle path were calculated over a 480-s period. A heat map showing the time spent in the entire chamber ([fig. 2B](#) and [supplementary fig. S1A, Supplementary Material](#) online) and a plot of the swimming speeds of the tadpoles ([fig. 2C](#) and [supplementary fig. S1B, Supplementary Material](#) online) were also produced using ANY-maze. If tadpoles continuously stopped moving for longer than approximately 1 min during the assay, the entire data set was omitted from analysis because we could not rule out the possibility that the tadpoles stayed in the same position due to reduced locomotor activity.

The purpose of the present study was to examine avoidance temperatures in tadpoles. Therefore, one side of the assay chamber (the test chamber) was heated or cooled, and the other side (the control chamber) was maintained close to rearing temperature (25–27 °C); however, the temperature of the control chamber also changed depending on the temperature of the test chamber (control vs. test chamber: 26 °C vs. 22 °C, 26 °C vs. 30 °C, 26 °C vs. 33 °C, 27 °C vs. 36 °C, 28 °C vs. 38 °C, 29 °C vs. 40 °C, 30 °C vs. 42 °C, 31 °C vs. 44 °C). For each thermal condition, the position of the test chamber was exchanged to minimize the potential effects of asymmetry. Temperatures at each end of the assay chamber fluctuated by approximately 1.5 °C from the set temperature due to the movement of the tadpoles during the assay. The avoidance index was calculated by subtracting the time spent in the test chamber from the time spent in the control chamber, and the resulting value was divided by the total assay time. The avoidance temperature of each species was defined as the temperature at which time the spent in the test chamber was significantly shorter than that spent in the control chamber, according to Welch's *t*-test ($P < 0.05$).

Tap water was purified using a charcoal filter and used for the temperature ramp and two-chamber choice assays (water pH 7.3–7.6). To examine the effect of CA in the two-chamber choice assay, 0.01 or 0.03 M stock solution of CA (dissolved in DMSO) was prepared and further diluted 1,000-fold with water. Thus, the final concentration of CA was 0.01 or 0.03 mM in the assay. For control experiments, an equivalent volume of DMSO was added to the water. For acidic conditions, water containing 0.5 mM 2-(*N*-morpholino)ethanesulfonic acid was adjusted to pH 7.0, 6.0, and 5.5 and used for the two-chamber choice assay.

Measurement of an Intracellular Calcium Ion in DRG Neurons

The preparation of DRG neurons from froglets and subsequent calcium imaging procedure were described in detail previously (Ohkita et al. 2012). Froglets were sacrificed by decapitation and isolated DRGs were enzymatically dissociated in Liebowitz-15 (Thermo Fisher Scientific, Waltham, MA, USA) tissue culture medium supplemented with collagenase P (2.5 mg/ml; Roche, Basel, Switzerland), dispase II (2 mg/ml; Roche), and DNase I (0.5 mg/ml; Roche) for 30 min at 37 °C. Following enzymatic digestion, the cells were mechanically dissociated using a fire-polished Pasteur pipette. The cell suspension was then centrifuged, and the resulting pellet was resuspended in culture medium. Aliquots were plated onto glass coverslips coated with poly-L-lysine (Sigma) in a humidified atmosphere at ~25 °C. The cells were used for the calcium imaging experiments within 1 day post preparation. To avoid bacterial contamination, 0.1% antibiotic solution (100 IU/mL penicillin G and 100 µg/ml streptomycin) was added to the culture medium.

[Ca²⁺]_i was measured using a fluorescent calcium indicator, fura-2, by dual excitation in a fluorescent imaging system

with software-controlled illumination and acquisition (Aqua Cosmos; Hamamatsu Photonics, Hamamatsu, Shizuoka, Japan), as described previously (Ohkita et al. 2012). The cells prepared from DRG were incubated for 40 min at 28 °C with 10 µM fura-2 acetoxymethyl ester (Fura-2 AM; Thermo Fisher Scientific) and 0.02% Cremophor EL (Merck, Kenilworth, NJ, USA) in HEPES-buffered solution containing the following (in mM): 103 NaCl, 6 KCl, 1.2 MgCl₂, 2.5 CaCl₂, 10 HEPES (pH 7.4 with NaOH). A coverslip attached with fura-2-loaded cells was placed in an experimental chamber mounted on the stage of an inverted microscope (IX71; Olympus, Tokyo, Japan) equipped with an image acquisition and analysis system. [Ca²⁺]_i was measured by exposing the cells to excitation wavelengths of 340 or 380 nm, and fluorescent intensity at 500 nm was recorded for each excitation wavelength. Basal temperature was maintained at room temperature (22–25 °C) in all experiments, and heat stimulation was applied by perfusing heated HEPES-buffered solution. DRG neurons in which the [Ca²⁺]_i increased above 50 nM during heat exposure were defined as heat-responsive neurons. Apparent thermal activation thresholds for heat-responsive DRG neurons were determined as the temperature at which the [Ca²⁺]_i reached 20% of the maximum increase during heat stimulation. Temperatures were monitored using a temperature sensor, which was located near the cells being observed, connected to a bridge pod (ML301; AD Instruments, Dunedin, New Zealand) together with an AD converter (PowerLab, AD Instruments).

Molecular Cloning of TRPV1 and TRPA1

TRPV1 and TRPA1 were cloned from *B. japonica*. Total RNA was extracted from a single *B. japonica* tadpole collected from Seranma hot spring on Kuchinoshima Island. The tadpole was soaked in RNAlater solution (Thermo Fisher Scientific) before use. Total RNA was extracted from the whole body using Sepaso[®]-RNA I Super G-for RNA (Nacalai Tesque, Kyoto, Japan). The reverse transcription reaction was performed with extracted total RNA as a template and oligo-dT primers to synthesize complementary DNA using the ReverTra Ace[®] (Toyobo, Osaka, Japan), according to the manufacturer's instructions. The PCR primers were designed according to the nucleotide sequences of TRPV1 or TRPA1 of *B. japonica* obtained by RNA sequencing analysis (Komaki et al. 2021). For TRPV1, the first round of PCR was performed using the reverse-transcribed products as the template with forward (5'-CATCAGAAGGAATCATTTTAAAGACTAGC-3') and reverse (5'-TGTTTGTATCCAACCTTACCAGTGTC-3') primers. Then, a second round of PCR was performed using the first PCR product as the template with forward (5'-taaggtagcATGAAGAAGATGGGAAGC-3', lower case letters indicate an attached sequence containing a restriction enzyme recognition site) and reverse (5'-taagcggcgcTTACAGAGGCTTATCTGTCC-3') primers. The DNA fragment containing the entire TRPV1 sequence was successfully obtained and cloned into pOX(+), an expression vector for *X. laevis* oocytes, using

a conventional cloning procedure. *KpnI* and *NotI* were used for cloning the TRPV1 DNA fragment into pOX(+). TRPA1 from *B. japonica* was also cloned using a similar procedure as described above. The primers used for the first round of PCR were (forward) 5'-GAAGAAGAAAAGAGTTTTGTCCAGTC-3' and (reverse) 5'-CAATTGAATATGGTGGATCTCTG-3', and those for the second round were (forward) 5'-taaggtaccATGAAGAAGTCAATTAGACG-3' and (reverse) 5'-taagcggccgcAAGAGCCAGCATTACTCC-3'. *KpnI* and *NotI* were used for cloning the TRPA1 DNA fragment into pOX(+).

To clone TRPV1 and TRPA1 from *B. buergeri*, total RNA was extracted from the whole body of a froglet collected from Hamamatsu, Shizuoka, Japan. The reverse transcription reaction was performed using oligo-dT primers and extracted total RNA as a template. The TRPV1-specific primers used for the first round of PCR were (forward) 5'-TTTAAGATTGGCTAATATGAAGAAGATGGG-3' and (reverse) 5'-CAGCAAACAAAAATATCGKCCCGGACAG-3', and those for the second round were (forward) 5'-taaggtaccATGAAGAAGATGGGAAGC-3' and (reverse) 5'-taagcggccgcTTACAGAGGCTTATCTGTCC-3'. TRPA1 was also cloned from *B. buergeri*. The primers used for the first round of PCR were (forward) 5'-GAAGAAGAAAAGAGTTTTGTCCAGTC-3' and (reverse) 5'-CAATTGAATATGGTGGATCTCTG-3', and those for the second round were (forward) 5'-taagaattcATGAAGAAGTCAATTAGACG-3' and (reverse) 5'-taagcggccgcAGTGCCAGCATCACTG-3'. The DNA fragment containing TRPV1 or TRPA1 was cloned into the pOX(+) vector using *KpnI/NotI* or *EcoRI/NotI*, respectively.

To clone TRPA1 from *Ra. japonica*, total RNA was extracted from a single tadpole collected from Higashi-Hiroshima, Hiroshima, Japan. The primers used for the first round of PCR were (forward) 5'-TGTGGACTCCACTGCACAACATGAAG-3' and (reverse) 5'-CAAA TACGATTGACCTTTATCATGCACAG-3', and those for the second round were (forward) 5'-atcggatccATGAA GAAATCAATCAGACG-3' and (reverse) 5'-catgcccgc TGCACAGAGACAGCATCAC-3'. The DNA fragment containing TRPA1 was cloned into the pOX(+) vector using *BamHI* and *NotI*. The nucleotide sequences of cloned TRPV1 or TRPA1 from all species were determined from multiple clones to confirm that no PCR errors were included.

Estimation of Relative Amount of TRPA1(V+) and TRPA1(V-)

Total RNA was extracted from whole tadpoles from *B. japonica*, *B. buergeri*, and *Ra. japonica* reared at room temperature (25–27°C). The reverse transcription reaction was performed with extracted total RNA as a template and oligo-dT primers to synthesize complementary DNA using the ReverTra Ace® (Toyobo) according to the manufacturer's instructions. RT-PCR was performed using the forward primer 5'-GAATTTGGGTTTAGTATTGAAGATCAATC-3' and the reverse primer 5'-ATGTAATGGTGTTCATTATTTCCATCTGG-3' for *B. japonica*. In *B. buergeri*, the forward primer 5'-GGATTGGATGTTTTCTATACACAT

GACTG-3' and the reverse primer 5'-ATGTAATGGTGTTCATTATTTCCATCTGG-3' were used for RT-PCR. In *Ra. japonica*, the first round of PCR was performed with the forward primers 5'-ATCGGATCCATGAAGAAATCAATCAGACG-3' and the reverse primer 5'-GCAATATCACCAACAGCCAGACCAATAAGC-3', and the second round of PCR was further performed using the forward primer 5'-GAA TTTGGGTTTAGTATTGAAGATCACATC-3' and the reverse primer 5'-GGCCAGCAGCAGAGGTGTACGA-3'. The amplified PCR products were directly sequenced, and signal intensities for TRPA1(V+) and TRPA1(V-) were measured at 14 nucleotide positions and the average values were obtained from each individual. The detail procedure for measuring signal intensities is shown in [supplementary fig. 3D](#) (Supplementary Material online).

Electrophysiological Assays

TRPA1 or TRPV1 was heterologously expressed in *X. laevis* oocytes, and ionic currents were recorded using a two-electrode voltage-clamp method (Saito et al. 2011). The pOX(+) vector harboring TRPV1 or TRPA1 was linearized using *MluI* and then used as the template for complementary RNA (cRNA) synthesis using the mMESSAGE MACHINE SP6 kit (Thermo Fisher Scientific) according to the manufacturer's instructions. Oocytes were excised from mature female *X. laevis*, and follicular membranes were enzymatically removed using collagenase A (Roche). cRNA (50 nl) was injected into defolliculated oocytes at a concentration of 50 or 100 ng/μl for TRPA1 and 200 or 300 ng/μl for TRPV1. Ionic currents were recorded 2–6 days post injection using the OC-725C amplifier (Warner Instruments, Holliston, MA, USA) with a 1 kHz low-pass filter and digitized at 5 kHz using the Digidata 1440 digitizer (Molecular Devices, San Jose, CA, USA). The oocytes were voltage-clamped at -60 mV. ND96 (in mM: 96 NaCl, 2 KCl, 1.8 CaCl₂, 1 MgCl₂, and 5 HEPES, pH 7.4) was used as the bath solution. Temperature was monitored using a thermistor located just beside the oocytes and the TC-344B dual channel temperature controller (Warner Instruments). Heated ND96 was perfused to apply heat stimulation. CA (Wako, Osaka, Japan) was dissolved in DMSO to prepare 0.003, 0.03, 0.1, 0.3, 1, 3, and 6 M stock solution, which were further diluted 1,000-fold with ND96 to prepare a working bath solution. For the acidic stimulation in [fig. 4](#), ND96 adjusted to pH 6.0, 5.5, or 5.0 was applied by perfusion. 2-(*N*-Morpholino)ethanesulfonic acid was used instead of HEPES to prepare ND96 adjusted to pH 6.0 or 5.5. For the acidic stimulation shown in [fig. 4A–C](#) or [4D–F](#), tri-sodium citrate dihydrate or 2-(*N*-morpholino) ethanesulfonic acid were used instead of HEPES to prepare ND96 adjusted to pH 5.0, respectively.

To examine the dose-dependent responses of TRPA1 to CA, current recordings were performed 2 or 3 days post injection. On the other hand, current recordings were conducted side-by-side at 2–4 days post injection to compare the heat-evoked activity of TRPA1 among the three species (three to five independent preparations).

Similarly, ionic currents were recorded at 4 or 6 days post injection to compare TRPV1 between the two *Buergeria* species (two independent preparations). Current recordings were performed side-by-side using oocytes prepared from a single frog when comparing their heat-evoked responses among the frog species, since the heat-evoked responses of *X. laevis* oocytes expressing TRPV1 or TRPA1 varied to some extent among the different preparations. Apparent thermal activation thresholds for TRPA1 were determined using *X. laevis* oocytes from multiple preparations (two or three independent preparations) by generating Arrhenius plots using Clampfit 10.4 (Molecular Devices) and Origin 9J (OriginLab, North Hampton, NH, USA) software. The EC₅₀ values for TRPA1(V-) to CA were obtained by fitting the plots obtained from each *Xenopus* oocytes applying a sigmoidal function using Origin 9J.

Statistical Analysis

Statistical significance was tested using Welch's *t*-test when comparing two groups and analysis of variance (ANOVA) followed by post-hoc unpaired *t*-test (with Bonferroni or Holm–Bonferroni correction), or by post-hoc Tukey's HSD test when comparing more than two groups. The Kruskal–Wallis test followed by the post-hoc Mann–Whitney *U* test with Bonferroni correction was also used to compare more than two groups in case when the variances among the groups were unequal. Statistical tests were performed using Origin 9J (OriginLab), Microsoft Excel 2019 (Microsoft, USA) and EZR 1.38 (Kanda 2013). Data are presented as means ± SE in the graphs unless otherwise noted.

Supplementary Material

Supplementary data are available at *Molecular Biology and Evolution* online.

Acknowledgments

The authors thank Keiko Fukuoka for maintenance of the tadpoles and Toshiyuki Sazi for constructing the thermo-regulator. The authors also thank the mayor of Toshima village, who granted permission for field observations and collection of *B. japonica* samples, and Eio Higo, Shimako Higo, and Kazuhiro Hidaka for their supporting with field research on Kuchinoshima Island. The authors thank Kiyomi Suzuki for his kind permission to conduct our field work and collect samples of *Ra. japonica* and *Rh. schlegelii*. This work was supported by grants-in-aid for Scientific Research (15H05927 to M.T. and 19K06797 and 22H02679 to S.S.) from the Ministry of Education, Culture, Sports, Science, and Technology of Japan.

Author Contributions

S.S. designed the study. T.I. and S.K. supplied the sequence data of TRPV1 and TRPA1 from *B. japonica* and *Ra.*

japonica. C.T.S. and S.S. cloned TRPA1 and TRPV1 and conducted electrophysiological experiments. T.O. and N.T. performed calcium imaging experiments using DRG neurons. S.S. performed the behavioral experiments. C.T.S. and S.S. analyzed the data. T.I., S.K., C.T.S., and S.S. performed the field research. S.S. and M.T. wrote the manuscript. All authors read and commented on the manuscript.

Data Availability

The nucleotide sequence data for *B. japonica* TRPA1, *B. japonica* TRPV1, *B. buergeri* TRPA1, *B. buergeri* TRPV1, and *Ra. japonica* TRPA1 were deposited into DDBJ/EMBL/GenBank under accession nos. LC603062, LC603063, LC603064, LC603065, and LC704439, respectively.

Conflict of interest statement. The authors declare no competing interests.

References

- Akashi HD, Saito S, Cadiz Diaz A, Makino T, Tominaga M, Kawata M. 2018. Comparisons of behavioural and Trpa1 heat sensitivities in three sympatric Cuban *Anolis* lizards. *Mol Ecol*. **27**:2234–2242.
- Angilletta MJ Jr, Youngblood JP, Neel LK, VandenBrooks JM. 2019. The neuroscience of adaptive thermoregulation. *Neurosci Lett*. **692**:127–136.
- Araujo MB, Ferri-Yanez F, Bozinovic F, Marquet PA, Valladares F, Chown SL. 2013. Heat freezes niche evolution. *Ecol Lett*. **16**:1206–1219.
- Bagriantsev SN, Gracheva EO. 2015. Molecular mechanisms of temperature adaptation. *J Physiol*. **593**:3483–3491.
- Caterina MJ, Leffler A, Malmberg AB, Martin WJ, Trafton J, Petersen-Zeit KR, Koltzenburg M, Basbaum AI, Julius D. 2000. Impaired nociception and pain sensation in mice lacking the capsaicin receptor. *Science*. **288**:306–313.
- Caterina MJ, Schumacher MA, Tominaga M, Rosen TA, Levine JD, Julius D. 1997. The capsaicin receptor: A heat-activated ion channel in the pain pathway. *Nature*. **389**:816–824.
- Chen T-C, Kam Y-C, Lin Y-S. 2001. Thermal physiology and reproductive phenology of *Buergeria japonica* (Rhacophoridae) breeding in a stream and a geothermal hot spring in Taiwan. *Zool Sci*. **18**:591–596.
- Dowland LK, Luyckx VA, Enck AH, Leclercq B, Yu AS. 2000. Molecular cloning and characterization of an intracellular chloride channel in the proximal tubule cell line, Llc-Pk1. *J Biol Chem*. **275**:37765–37773.
- Fukuyama K, Kusano T. 1992. Factors affecting breeding activity in a stream-breeding frog, *Buergeria-Buergeri*. *J Herpetol*. **26**:88–91.
- Gavva NR, Klionsky L, Qu Y, Shi L, Tamir R, Edenson S, Zhang TJ, Viswanadhan VN, Toth A, Pearce LV, et al. 2004. Molecular determinants of vanilloid sensitivity in Trpv1. *J Biol Chem*. **279**:20283–20295.
- Glauser DA, Goodman MB. 2016. Molecules empowering animals to respond to temperature in changing environments. *Curr Opin Neurobiol*. **41**:92–98.
- Gosner KL. 1960. A simplified table for staging anuran embryos and larvae with notes on identification. *Herpetologica*. **16**:183–190.
- Jabba S, Goyal R, Sosa-Pagan JO, Moldenhauer H, Wu J, Kalmeta B, Bandell M, Latorre R, Patapoutian A, Grandl J. 2014. Directionality of temperature activation in mouse Trpa1 ion channel can be inverted by single-point mutations in ankyrin repeat six. *Neuron*. **82**:1017–1031.
- Jordt SE, Julius D. 2002. Molecular basis for species-specific sensitivity to “hot” chili peppers. *Cell*. **108**:421–430.

- Jordt SE, Tominaga M, Julius D. 2000. Acid potentiation of the capsaicin receptor determined by a key extracellular site. *Proc Natl Acad Sci U S A*. **97**:8134–8139.
- Julius D. 2013. Trp channels and pain. *Annu Rev Cell Dev Biol*. **29**: 355–384.
- Kanda Y. 2013. Investigation of the freely available easy-to-use software 'ezr' for medical statistics. *Bone Marrow Transplant*. **48**: 452–458.
- Komaki S, Igawa T, Lin SM, Sumida M. 2016. Salinity and thermal tolerance of Japanese stream tree frog (*Buergeria japonica*) tadpoles from island populations. *Herpetol J*. **26**:207–211.
- Komaki S, Lau Q, Igawa T. 2016. Living in a Japanese onsen: field observations and physiological measurements of hot spring amphibian tadpoles, *Buergeria japonica*. *Amphib Reptil*. **37**:311.
- Komaki S, Matsunami M, Lin JW, Lee KH, Lin YP, Lee Y, Lin SM, Igawa T. 2021. Transcriptomic changes in hot spring frog tadpoles (*Buergeria otai*) in response to heat stress. *Front Ecol Evol*. **9**: 706887.
- Komaki S, Sutoh Y, Kobayashi K, Saito S, Saito CT, Igawa T, Lau Q. 2020. Hot spring frogs (*Buergeria japonica*) prefer cooler water to hot water. *Ecol Evol*. **10**:9466–9473.
- Kumar S, Stecher G, Suleski M, Hedges SB. 2017. Timetree: A resource for timelines, timetrees, and divergence times. *Mol Biol Evol*. **34**: 1812–1819.
- Kurganov E, Zhou Y, Saito S, Tominaga M. 2014. Heat and airtc activate green anole Trpa1 in a membrane-delimited manner. *Pflugers Arch*. **466**:1873–1884.
- Laing RJ, Dhaka A. 2016. Thermotrp and pain. *Neuroscientist* **22**: 171–187.
- Laursen WJ, Anderson EO, Hoffstaetter LJ, Bagriantsev SN, Gracheva EO. 2015. Species-specific temperature sensitivity of Trpa1. *Temperature (Austin)* **2**:214–226.
- Laursen WJ, Schneider ER, Merriman DK, Bagriantsev SN, Gracheva EO. 2016. Low-cost functional plasticity of Trpv1 supports heat tolerance in squirrels and camels. *Proc Natl Acad Sci U S A*. **113**:11342–11347.
- Matsui M, Tominaga A. 2020. A new species of *Buergeria* from the Southern Ryukyus and Northwestern Taiwan (Amphibia: Rhacophoridae). *Curr Herpetol*. **39**:160–172.
- Ohkita M, Saito S, Imagawa T, Takahashi K, Tominaga M, Ohta T. 2012. Molecular cloning and functional characterization of *Xenopus tropicalis* frog transient receptor potential vanilloid 1 reveal its functional evolution for heat, acid, and capsaicin sensitivities in terrestrial vertebrates. *J Biol Chem*. **287**:2388–2397.
- Patapoutian A, Peier AM, Story GM, Viswanath V. 2003. Thermotrp channels and beyond: mechanisms of temperature sensation. *Nat Rev Neurosci*. **4**:529–539.
- Paulsen CE, Armache JP, Gao Y, Cheng Y, Julius D. 2015. Structure of the Trpa1 ion channel suggests regulatory mechanisms. *Nature* **520**:511–517.
- Perez-Escudero A, Vicente-Page J, Hinz RC, Arganda S, de Polavieja GG. 2014. Idtracker: tracking individuals in a group by automatic identification of unmarked animals. *Nat Methods* **11**:743–748.
- Rosenzweig M, Brennan KM, Tayler TD, Phelps PO, Patapoutian A, Garrity PA. 2005. The *Drosophila* ortholog of vertebrate Trpa1 regulates thermotaxis. *Genes Dev*. **19**:419–424.
- Ryu S, Liu B, Yao J, Fu Q, Qin F. 2007. Uncoupling proton activation of vanilloid receptor Trpv1. *J Neurosci*. **27**:12797–12807.
- Saito S, Banzawa N, Fukuta N, Saito CT, Takahashi K, Imagawa T, Ohta T, Tominaga M. 2014. Heat and noxious chemical sensor, chicken Trpa1, as a target of bird repellents and identification of its structural determinants by multispecies functional comparison. *Mol Biol Evol*. **31**:708–722.
- Saito S, Fukuta N, Shingai R, Tominaga M. 2011. Evolution of vertebrate transient receptor potential vanilloid 3 channels: opposite temperature sensitivity between mammals and western clawed frogs. *PLoS Genet*. **7**:e1002041.
- Saito S, Nakatsuka K, Takahashi K, Fukuta N, Imagawa T, Ohta T, Tominaga M. 2012. Analysis of transient receptor potential ankyrin 1 (Trpa1) in frogs and lizards illuminates both nociceptive heat and chemical sensitivities and coexpression with trp vanilloid 1 (Trpv1) in ancestral vertebrates. *J Biol Chem*. **287**: 30743–30754.
- Saito S, Ohkita M, Saito CT, Takahashi K, Tominaga M, Ohta T. 2016. Evolution of heat sensors drove shifts in thermosensation between *Xenopus* species adapted to different thermal niches. *J Biol Chem*. **291**:11446–11459.
- Saito S, Saito CT, Nozawa M, Tominaga M. 2019. Elucidating the functional evolution of heat sensors among *Xenopus* species adapted to different thermal niches by ancestral sequence reconstruction. *Mol Ecol*. **28**:3561–3571.
- Saito S, Tominaga M. 2015. Functional diversity and evolutionary dynamics of thermotrp channels. *Cell Calcium*. **57**:214–221.
- Saito S, Tominaga M. 2017. Evolutionary tuning of Trpa1 and Trpv1 thermal and chemical sensitivity in vertebrates. *Temperature (Austin)* **4**:141–152.
- Sunday JM, Bates AE, Dulvy NK. 2011. Global analysis of thermal tolerance and latitude in ectotherms. *Proc Biol Sci*. **278**: 1823–1830.
- Sunday JM, Bates AE, Dulvy NK. 2012. Thermal tolerance and the global redistribution of animals. *Nat Clim Change*. **2**:686–690.
- Tominaga M, Caterina MJ, Malmberg AB, Rosen TA, Gilbert H, Skinner K, Raumann BE, Basbaum AI, Julius D. 1998. The cloned capsaicin receptor integrates multiple pain-producing stimuli. *Neuron* **21**:531–543.
- Tominaga A, Matsui M, Eto K, Ota H. 2015. Phylogeny and differentiation of wide-ranging Ryukyu Kajika frog *Buergeria japonica* (Amphibia: Rhacophoridae): geographic genetic pattern not simply explained by vicariance through strait formation. *Zoolog Sci*. **32**:240–247.
- Vandewauw I, De Clercq K, Mulier M, Held K, Pinto S, Van Ranst N, Segal A, Voet T, Vennekens R, Zimmermann K, et al. 2018. A trp channel trio mediates acute noxious heat sensing. *Nature* **555**:662–666.
- Viswanath V, Story GM, Peier AM, Petrus MJ, Lee VM, Hwang SW, Patapoutian A, Jegla T. 2003. Opposite thermosensor in fruitfly and mouse. *Nature* **423**:822–823.
- Wang YH, Hsiao YW, Lee KH, Tseng HY, Lin YP, Komaki S, Lin SM. 2017. Acoustic differentiation and behavioral response reveals cryptic species within *Buergeria* treefrogs (Anura, Rhacophoridae) from Taiwan. *PLoS One* **12**:e0184005.
- Wu C-S, Kam Y-C. 2005. Thermal tolerance and thermoregulation by Taiwanese rhacophorid tadpoles (*Buergeria japonica*) living in geothermal hot springs and streams. *Herpetologica* **61**:35–46.
- Yang S, Lu X, Wang Y, Xu L, Chen X, Yang F, Lai R. 2020. A paradigm of thermal adaptation in penguins and elephants by tuning cold activation in Trpm8. *Proc Natl Acad Sci U S A*. **117**:8633–8638.